# State-Space Models and Particle Filters

Edoardo Marcelli    Roberto Colarieti    Alexei Verkhovtsev    Michele Bolla

Gabriele Romano    Benedetta Bruni

31 luglio, 2021

# Introduction

State-Space models represent an extremely interesting class of models and they are used extensively, for instance, for inference and forecasting in time-series and macroeconometric analysis. In fact, they allow to model observational data as function of underlying states that cannot be observed. For instance, in macroeconomic models GDP is usually observed while the TFP sequence is the hidden state determining output. In this work we describe techniques, such as Kalman and Particle filter, that allows to approximate probability distributions for the states from the observed data. For example, from the sequence of observed GDP, it is possible to "filter" the TFP factor.

Furthermore, it is possible to impose a Markov structure to State-Space models, assuming that the states are Markov, i.e., the probability of the current state depends on the entire sequence of past states only through its first lag. The combination of State-Space and Markov structures constitutes a powerful modeling assumption for inference and forecasting.

Withing the Monte Carlo (MC) methods, where inference is based on repeated simulations that allow to approximate the target distributions (needed to compute the estimator of interest), Particle Filter (PF) Algorithms represent the most important class of procedures for State-Space-Markov models. PF allows to sample states period-by-period, updating sequentially the filtering distributions (i.e., the distribution of current state conditional on all the sequence of observations - up to the current period one -), incorporating the information on the likelihood of the extracted states given the sequence of observations, by means of re-weighting.

Moreover, the PF is a very general algorithm, since it can be applied to non-linear models with non-Gaussian errors, while it does not allow for a closed form solution. On the contrary, the Kalman Filter, is a filtering method that can be applied in the case of linear-Gaussian State-Space-Markov models, that remains analytically tractable. In this work we will describe both these algorithms, while our main focus remains on Particle Filter. In chapter 1 we define precisely Markov processes and State-Space Models. In chapter 2 we describe the

Kalman Filter and in chapter 3 we analyze extensively the Particle Filter. Finally, in chapter 4, we apply these methods to stochastic volatility models.

Finally, we find it useful to integrate each section where an algorithm is described and analyzed from a theoretical perspective with an implementation subsection, using as an example a simple Random-Walk State-Space model. In this way, the reader can visualize the codes and the practical meaning of the Kalman and Particle Filter algorithms, immediately after their theoretical description.

# Chapter 1

# Markov Processes and State-Space Models

## 1.1 Notation

Let us fix the basic notation that will be employed henceforth. Upper case letters, e.g. $X_t, Y_t$, denote random variables, while lower case letters denote the realizations. Finite sequences are made compact using the semi-colon notation, e.g. $x_{0:t} = (x_0, x_1, \ldots, x_t)$ for some $t \geq 0$. The sets of outcomes are denoted by upper case calligraphic letters, e.g. $\mathcal{X}, \mathcal{Y}$. The $\sigma$-algebra of a set $\mathcal{X}$ reads $\mathcal{B}(\mathcal{X})$. The pair $(\mathcal{X}, \mathcal{B}(\mathcal{X}))$ is a measurable space. The densities are represented with lower case cursive letters. For example, the density of $X_t$ in $x_t$ is $p_t^\theta(x_t)$, where $\theta \in \Theta$ is some (eventually known) vector, while the density of $X_t$ in $x_t$, given that $X_{t-1}$ has previously taken value $x_{t-1}$, is $p_t^\theta(x_t \mid x_{t-1})$. Note that $p_t^\theta(x_t \mid x_{t-1})$ is a member of the parametric family with parameters $(\theta, x_{t-1})$. The probability distribution of a random variable $X_t$ is represented by $\mathbb{P}_t(dx_t)$, while the probability distribution of a sequence $X_{0:t}$ is represented by $\mathbb{P}_t(dx_{0:t})$. The Dirac measure, i.e., the measure that assigns probability 1 to the singleton $\{x\}$, is denoted by $\delta_x(dy)$. The expectation operator is denoted by $\mathbb{E}$, where the section of $\mathbb{E}$ at $\mathbb{Q}$, i.e., $\mathbb{E}_\mathbb{Q}$ denotes the operator computed with respect to the probability distribution $\mathbb{Q}$. Let $\varphi$ be a function defined on the random variable $X \propto \mathbb{Q}$. Then, we denote the expected value of $\varphi(X)$ with

$$\mathbb{E}_\mathbb{Q}[\varphi(X)] = \int_\mathcal{X} \varphi(x) \mathbb{Q}(dx).$$

3

Convergence in distribution is denoted with the symbol $\implies$ . So, $X \implies \mathcal{N}(0, 1)$ means that the random variable $X$ converges in distribution to a normal Gaussian.

## 1.2 Markov Processes

Let $(\mathcal{X}, \mathcal{B}(\mathcal{X}))$ and $(\mathcal{Y}, \mathcal{B}(\mathcal{Y}))$ be two (eventually equal) measurable spaces.
**Definition 1**

*A function $P(x, dy) : (\mathcal{X}, \mathcal{B}(\mathcal{X})) \to [0, 1]$ such that*

- *for all $x \in \mathcal{X}, P(x, \cdot)$ is a probability measure on $(\mathcal{Y}, \mathcal{B}(\mathcal{Y}))$, and*

- *for all subsets $A \in \mathcal{B}(\mathcal{Y})$, the map $x \mapsto P(x, A)$ is measurable in $\mathcal{B}(\mathcal{X}))$,*

*is defined a probability kernel from $(\mathcal{X}, \mathcal{B}(\mathcal{X}))$ to $(\mathcal{Y}, \mathcal{B}(\mathcal{Y}))$.*

Notice that for any random variables $X_1$ and $X_0 = x_0$,

$$\mathbb{P}_1(dx_{0:1}) = \mathbb{P}_0(dx_0)P_1(x_0, dx_1),$$

where $P_1(x_0, dx_1)$ is a probability kernel from $(\mathcal{X}, \mathcal{B}(\mathcal{X}))$ to $(\mathcal{X}, \mathcal{B}(\mathcal{X}))$. This remark, provides some intuition about the link between probability kernels and conditional probabilities. As a matter of fact, it is possible to show that for given $X_{0:1}$ with joint probability distribution $\mathbb{P}_1(dx_{0:1})$,

$$\mathbb{P}_1(X_1 \in dx_1 \mid X_0 = x_0) = P_1(x_0, dx_1). \tag{1.1}$$

Probability kernels can be used to define Markov processes. Before moving to the definition, we will introduce some important concepts. Recall that given two measures $\mathbb{M}$ and $\mathbb{Q}$ defined on a measurable space $(\mathcal{X}, \mathcal{B}(\mathcal{X}))$, $\mathbb{Q}$ is absolutely continuous with respect to $\mathbb{M}$, that is $\mathbb{Q} \ll \mathbb{M}$, if for all sets $A \in \mathcal{B}(\mathcal{X})$ such that $\mathbb{M}(A) = 0$, then it must also hold that $\mathbb{Q}(A) = 0$. If $\mathbb{Q}(A)/\mathbb{M}(A)$ is well-defined for all $A$, then the Radon-Nikodym theorem guarantees that there exists a measurable function $w(x) \geq 0$ such that

$$w(x) = \frac{\mathbb{Q}(dx)}{\mathbb{M}(dx)},$$

meaning that,

$$\mathbb{Q}(A) = \int_A w(x)\mathbb{M}(dx).$$

Let $P_1, P_2, \ldots, P_T$ be a finite sequence of probability kernels from $(\mathcal{X}, \mathcal{B}(\mathcal{X}))$ to $(\mathcal{X}, \mathcal{B}(\mathcal{X}))$. Fix some $\mathbb{P}_0(dx)$ on $(\mathcal{X}, \mathcal{B}(\mathcal{X}))$.

**Definition 2**

*A discrete-time Markov process is a sequence $X_{0:T}$ of random variables whose joint distribution can be written as*

$$\mathbb{P}_T(X_{0:T} \in dx_{0:T}) = \mathbb{P}_0(dx_0) \prod_{s=1}^{T} P_s(x_{s-1}, dx_s). \tag{1.2}$$

*The set $\mathcal{X}$ is the state-space, $\mathbb{P}_0$ is the initial distribution and the probability kernel $P_t$ is the transition kernel.*

It is possible to show that for any $t \in T$,

$$\mathbb{P}_T(X_t \in dx_t \mid X_{0:t-1} \in dx_{0:t-1}) = \mathbb{P}_T(X_t \in dx_t \mid X_{t-1} = x_{t-1}) = P_t(x_{t-1}, dx_t).$$

The first equality implies conditional independence. The second equality implies that it is possible to identify conditional distributions with transition kernels. Assume $\mathbb{P}_t$, with $t \leq T$, is a sequence of probability measures. Then, the following proposition holds.

**Proposition 1**

*For all $t \leq T$,*

$$\mathbb{P}_T(dx_{0:t}) = \mathbb{P}_0(dx_0) \prod_{s=1}^{t} P_s(x_{s-1}, dx_s) = \mathbb{P}_t(dx_{0:t}).$$

This means that the marginal distribution of $X_{0:t}$ with respect to $\mathbb{P}_T$ is $\mathbb{P}_t$.

## 1.3  State-Space Models

We now define *State-Space models* as Markov processes that are partially observed. Let $X_t \in \mathcal{X}$ and $Y_t \in \mathcal{Y}$ and let $\{(X_t, Y_t)\}$ be a stochastic process. To help intuition, suppose that $\{Y_t\}$ is observable, i.e., coincides with a sequence of observations, while $\{X_t\}$ is latent. Consider the initial distribution $\mathbb{P}_0(dx_0)$ and the probability kernels $P_t(x_{t-1}, dx_t)$ and $F_t(x_t, d_t)$, where $t = 1, 2, \dots$.

**Definition 3**

*The process $\{(X_t, Y_t)\}$ is a State-Space model if the joint distribution of $(X_{0:T}, Y_{0:T})$ is*

$$\begin{aligned}
\mathbb{P}_T(X_{0:T} \in dx_{0:T}, Y_{0:T} \in dy_{0:T}) &= \mathbb{P}_0(dx_0) \prod_{t=1}^{T} P_t(x_{t-1}, dx_t) \prod_{t=1}^{T} F_t(x_t, dy_t) \\
&= [\mathbb{P}_0(dx_0) F_0(x_0, y_0)] \prod_{t=1}^{T} [P_t(x_{t-1}, dx_t) F_t(x_t, dy_t)] \\
&= \mathbb{P}_T(dx_{0:T}) \prod_{t=1}^{T} F_t(x_t, dy_t).
\end{aligned}$$

From the second inequality, it is apparent that $\{(X_t, Y_t)\}$ is a Markov process with initial distribution $[\mathbb{P}_0(dx_0)F_0(x_0, y_0)]$ and transition kernel $P_t(x_{t-1}, dx_t)F_t(x_t, dy_t)$. The third equality, instead, shows that, $\{X_t\}$ has a marginal distribution

$$\mathbb{P}_T(dx_{0:T}) = \mathbb{P}_0(dx_0) \prod_{t=1}^{T} P_t(x_{t-1}, dx_t),$$

meaning that $\{X_t\}$ is marginally distributed as a Markov process with initial distribution $\mathbb{P}_T(dx_{0:T})$ and transition kernel $P_t(x_{t-1}, dx_t)$.

Assume now that there exists a dominating measures $\nu(dy)$ such that $F_t(x_t, dy_t) = f_t(y_t \mid x_t)\nu(dy_t)$ for all $t$. Then by the last equality of definition 3, the joint distribution of $(X_{0:T}, Y_{0:T})$ is

$$\mathbb{P}_T(X_{0:T} \in dx_{0:T}, Y_{0:T} \in dy_{0:T}) = \mathbb{P}_T(dx_{0:T}) \prod_{t=0}^{T} f_t(y_t \mid x_t) \prod_{t=0}^{T} \nu(dy_t). \tag{1.3}$$

Integrating away $X_{0:T}$, one gets the marginal density

$$\mathbb{P}_T(dy_{0:T}) = \mathbb{E}_{\mathbb{P}_t}\Big[ \prod_{s=0}^{t} f_s(y_s \mid X_s) \Big] \prod_{s=0}^{t} \nu(dy_s) = p_t(y_{0:t}) \prod_{s=0}^{t} \nu(dy_s), \tag{1.4}$$

where $p_t(y_{0:t})$ is the likelihood function. Dividing the left-hand side of equation 1.3 by the left-hand side of equation 1.4 and the right-hand side of equation 1.3 by the right-hand side of equation 1.4, one obtains the distribution

$$\mathbb{P}_t(X_{0:t} \in dx_{0:t} \mid Y_{0:t} = y_{0:t}) = \frac{1}{p_t(y_{0:t})} \Big[ \prod_{s=0}^{t} f_s(y_s \mid X_s) \Big] \mathbb{P}_t(dx_{0:t}). \tag{1.5}$$

# Chapter 2

# Linear-Gaussian case

*Linear Gaussian models* are a class of popular state-space models. A notable property of such models is that the filtering and predictive distributions are analytically tractable, which makes such models very convenient in applications.

Suppose that $\mathcal{X} = \mathbb{R}^{d_x}$ and $\mathcal{Y} = \mathbb{R}^{d_y}$. Let $U_t \sim \mathcal{N}(0, \Sigma_t)$ and $V_t \sim \mathcal{N}(0, \Lambda_t)$ be two independent white-noise errors and assume the initial distribution $X_0 \sim \mathcal{N}(0, \Sigma_0)$. We have a linear Gaussian model if

$$X_t = A_t X_{t-1} + U_t \tag{2.1}$$

$$Y_t = B_t X_t + V_t. \tag{2.2}$$

Note that $X_t \mid X_{t-1}$ and $Y_t \mid X_t$ are both normally distributed.

**Lemma 1**

*Let $X \sim \mathcal{N}(m_0, C_0)$ and $Y \mid X \sim \mathcal{N}(BX, \Lambda)$, where R and $Q_0$ are positive semi-definite matrices. Then, it holds that*

$$X \mid Y = y \sim \mathcal{N}(m_1, C_1), \tag{2.3}$$

$$C_1 = C_0 \left( I_{d_x} - B'(BC_0B' + \Lambda)^{-1} BC_0 \right) \tag{2.4}$$

$$m_1 = \left[ I_{d_x} - C_0 B'(BC_0B' + \Lambda)^{-1} B \right] m_0 + C_0 B'(BC_0B' + \Lambda)^{-1} y. \tag{2.5}$$

**Proof.** *The lemma can be proved using Bayes' Theorem. Suppose $X \sim \mathcal{N}(m_0, C_0)$. It is easy to see that*

$$p(x) \propto exp\left( -\frac{1}{2} x' C_0^{-1} x + x' C_0^{-1} m_0 \right). \tag{2.6}$$

7

*Now, by Bayes' Theorem,*

$$p(x \mid Y = y) \propto p(x)p(y \mid x)$$

$$\propto exp\left(-\frac{1}{2}x'C_0^{-1}x + x'C_0^{-1}m_0 - \frac{1}{2}(y - Bx)'\Lambda^{-1}(y - Bx)\right)$$

$$\propto exp\left(-\frac{1}{2}x'C_0^{-1}x + x'C_0^{-1}m_0 - \frac{1}{2}x'B'\Lambda^{-1}Bx + x'B'\Lambda^{-1}y\right)$$

$$= exp\left(-\frac{1}{2}x'(C_0^{-1} + B'\Lambda^{-1}B)x + x'(C_0^{-1}m_0 + B'\Lambda^{-1}y)\right).$$

*Hence, it follows that*

$$C_1 = Var(X \mid Y = y) = (C_0^{-1} + B'\Lambda^{-1}B)^{-1} = C_0 - C_0B'(BC_0B' + \Lambda)^{-1}BC_0$$

*and*

$$m_1 = \mathbb{E}(X \mid Y = y) = C_1^{-1}(C_0^{-1}m_0 + B'\Lambda^{-1}y)$$

$$= (C_0 - C_0B'(BC_0B' + \Lambda)^{-1}BC_0)(C_0^{-1}m_0 + B'\Lambda^{-1}y)$$

$$= m_0 - C_0B'(BC_0B' + \Lambda)^{-1}Bm_0 + C_0B'\Lambda^{-1}y - C_0B'(BC_0B' + \Lambda)^{-1}BC_0B'\Lambda^{-1}y$$

$$= [I_{d_x} - C_0B'(BC_0B' + \Lambda)^{-1}B]m_0 + C_0B'(BC_0B' + \Lambda)^{-1}y.$$

■

Assume that $\mathbb{P}_{t-1}(dx_{t-1} \mid Y_{1:t-1} = y_{1:t-1}) = \mathcal{N}(m_{t-1}, C_{t-1})$. Then, using the transition equation of the latent variable, by the linearity of the Gaussian distribution, we have that the predictive distribution is

$$\mathbb{P}_{t-1}(dx_t \mid Y_{1:t-1} = y_{1:t-1}) = \mathcal{N}(A_t m_{t-1}, A_t C_{t-1} A_t' + \Sigma_t). \tag{2.7}$$

Letting $R_T = A_t C_{t-1} A_t' + \Sigma_t$, and applying lemma 1, it follows that the filtering distribution is

$$\mathbb{P}_t(X_t \in dx_t \mid Y_{1:t-1} = y_{1:t-1}) = \mathcal{N}(m_t, C_t), \text{ where}$$

$$C_t = R_t[I_{d_x} - B_t'(B_t R_t B_t' + \Lambda_t)^{-1}B_t R_t]$$

$$m_t = [I_{d_x} - R_t B_t'(B_t R_t B_t' + \Lambda_t)^{-1}B_t]A_t m_{t-1} + R_t B_t'(B_t R_t B_t' + \Lambda_t)^{-1}y_t.$$

In some situations, it is possible to linearize otherwise non-linear models in order to employ this filtering method. There are, however, cases where this is not possible or where the linearization is not satisfactory. One such example is the stochastic volatility model. In the following chapters, we will introduce powerful algorithms that can be used in much more general settings.

## 2.0.1 Implementation

The aim of this subsection is to provide a practical illustration of the algorithms discussed in the main chapters. For the sake of simplicity we use for implementations a random walk plus noise model, i.e. the most basic form of linear Gaussian state-space model.

$$y_t|x_t \sim N(x_t, \sigma^2) \tag{2.8}$$

$$x_t|x_{t-1} \sim N(x_{t-1}, \tau^2) \tag{2.9}$$

$$x_0 \sim N(m_0, C_0) \tag{2.10}$$

As already mentioned before, in this case the filtering distribution can be computed in closed form solutions using the Kalman filter. However, this toy example will be used also to illustrate more involved filtering strategies described in this work. We believe indeed that it represents a useful starting point to understand the logic of the algorithms which may be eventually replicated when dealing with more complex models.

The filtering strategy is applied to 50 simulated data. Figure 2.1 shows the simulated true states sequence assuming as data generating process the Equation (2.9) with $\tau^2 = 1$ and simulated observed sequence process form Equation (2.8) with $\sigma^2 = 1$.
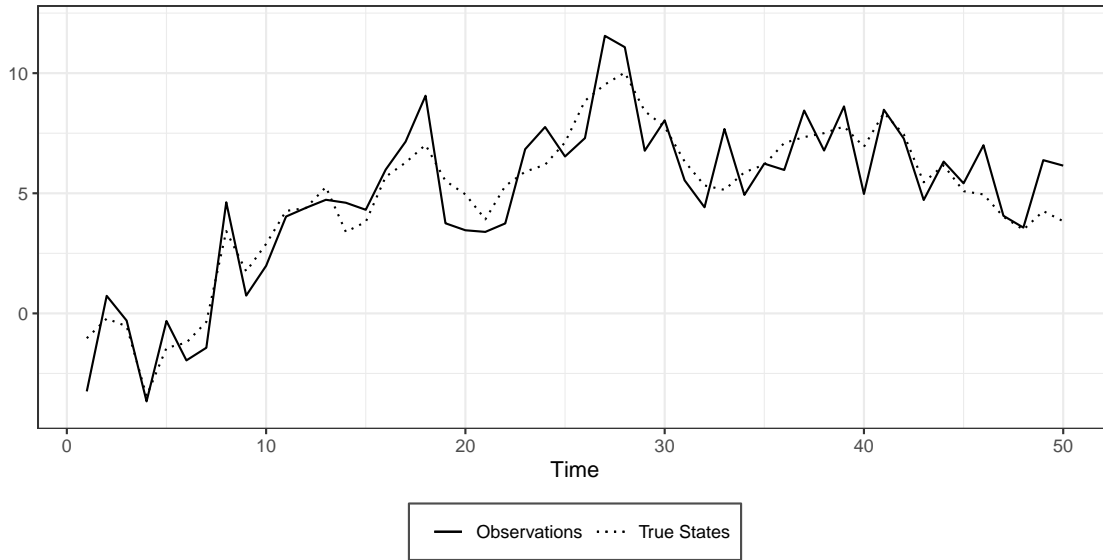


Figure 2.1: Simulated random walk plus noise model

The Kalman Filter for this model is implemented as described below.

**Algorithm** *Kalman Filter for Random Walk plus Noise Model*

- *Initialize $x_0 \sim N(m_0, C_0)$*

- *For $t = 1, ..., n$:*

    1. *Compute the one-step-ahead state predictive distribution at time $t - 1$, notice that if $t = 1$ no data have been observed yet and therefore $x_1|x_0 \sim N(a_1, R_1)$ otherwise*

    $$x_t|y_{1:t-1} \sim N(a_t, R_t)$$

    $$a_t = m_{t-1}$$

    $$R_t = C_{t-1} + \tau^2$$

    2. *Compute the filtering distribution at time $t$ as $p(x_t|y_{1:t}) \propto p(x_t|y_{1:t-1})p(y_t|x_t)$, i.e. the product of the one-step-ahead state predictive distribution and the likelihood*

    $$x_t|y_{1:t} \sim N(m_t, C_t)$$

    $$m_t = \left(1 - \frac{R_t}{R_t + \sigma^2}\right)a_t + \frac{R_t}{R_t + \sigma^2}y_t$$

    $$C_t = \frac{R_t}{R_t + \sigma^2}\sigma^2$$

Our `DLM` function implement in R replicate this steps.

---

```
DLM(data,sig2,tau2,m0,C0)
```

---

**Arguments**

`data`   the observed process. It has to be a vector or a univariate time series.

`sig2`   the variance $\sigma^2$ in observation equation

`tau2`   the variance $\tau^2$ in state equation

`m0`   central value of the normal prior state distribution

`C0`   variance of the normal prior state distribution

```r
DLM<-function(data,sig2,tau2,m0,C0){
  n  = length(data)
  m  = rep(0,n)
  C  = rep(0,n)
  for (t in 1:n){
```

```
    if (t==1){
       a = m0
       R = C0 + tau2
    }else{
       a = m[t-1]
       R = C[t-1] + tau2
    }
    A = R/(R+sig2)
    m[t] = (1-A)*a + A*y[t]
    C[t] = A*sig2
  }
  return(list(m=m,C=C))
}
```

In Figure 2.2 below filtered states estimated using Kalman Filter with $x_0 \sim N(0, 100)$ and $\sigma^2 = \tau^2 = 1$ are compared to the true states values. Notice how closely the filtered states follow the observations and the goodness of the approximation of the true states. 95 percent credible intervals are computed as

$$[E(x_t|y_{1:t}) - z_{1-\alpha/2} \sqrt{V(x_t|y_{1:t})}, E(x_t|y_{1:t}) + z_{1-\alpha/2} \sqrt{V(x_t|y_{1:t})}]$$
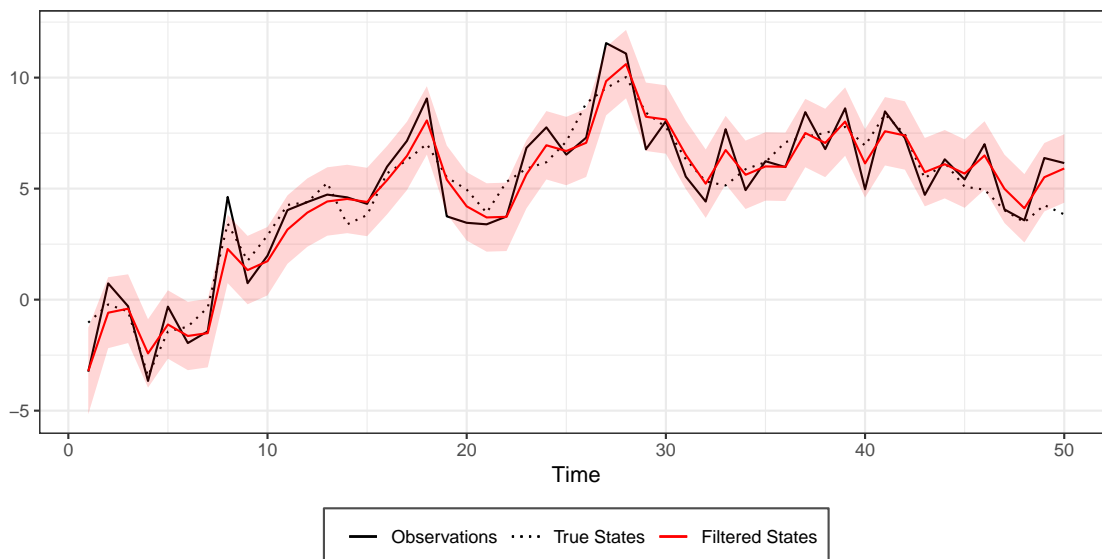


Figure 2.2: Kalman Filtered States with credible interval (in red)

The discussion of Kalman Filter will continue in the next sections where we compare it to the Particle Filter.

# Chapter 3

# Particle Filter

In the previous chapter we explained how the Kalman Filter is applied to the case of a linear model with Gaussian errors to find closed-form solution for the filtering and the predictive distributions. Nonetheless, the majority of time-series models have a non-linear structure and errors might follow non-Gaussian distributions. In this chapter we describe *particle filter* as an algorithm that allows to update sequentially the filtering and the predictive distributions in the non-linear and non-Gaussian case. Additionally, the Kalman Filter can be seen as a special case of the more general particle filter.

In section 3.1 we introduce the fundamental notions of *importance sampling*, *sequential importance sampling* and *resampling*. Then, in section 3.2 we describe three particle filtering algorithms: the *bootstrap*, the *guided* and the *auxiliary particle filters*. Instead, in section 3.3 we describe the *Liu and West filter*, when particle filtering is used to estimate model's parameters. Finally, in section 3.4 we establish some general convergence results for Particle Filter - Monte Carlo estimators.

## 3.1   Introductory notions: sampling and resampling

Let $\varphi : \mathcal{X} \to \mathbb{R}$ be a measurable, integrable and bounded real-valued function, where $(\mathcal{X}, \mathcal{B}(\mathcal{X}), \mathbb{Q})$ is a probability space.[1] Suppose that the probability measure $\mathbb{Q}$ admits a density $q(x)$ with respect to some measure $\nu(dx)$ and it is feasible to sample from that density.

To estimate the expected value of $\varphi$ with respect to the density $q$, the basic Monte Carlo (MC) method would require to sample $N$ times from the target density $q$ and to compute the average of the function $\varphi$ values. $\hat{\varphi}_{MC}$

---

[1]$\mathcal{B}(\mathcal{X})$ is the Borel sigma-algebra of $\mathcal{X}$.

is the standard MC estimator:

$$\hat{\varphi}_{MC} = \frac{1}{N} \sum_{n=1}^{N} \varphi(X^n) \approx \mathbb{E}_q(\varphi) \quad X^n \sim q(\cdot)$$

However, in many circumstances either it is impossible to sample from the target density or there exist another density - call it $m(\cdot)$ - different from $q$ that produces "more efficient" estimates. In all the cases for which sampling takes place from a distribution different from the "correct" (i.e., the true) one, importance sampling and resampling methods can be applied (as augmented versions of the standard MC algorithm).

### 3.1.1 Importance sampling

Let us consider two probability spaces: $(\mathcal{X}, \mathcal{B}(\mathcal{X}), \mathbb{Q})$ and $(\mathcal{X}, \mathcal{B}(\mathcal{X}), \mathbb{M})$ and let the measurable function $w : \mathcal{X} \to \mathbb{R}$ be proportional to the Radom-Nikodym derivative between $\mathbb{Q}$ and $\mathbb{M}$, i.e., $w(x) \propto \frac{\mathbb{Q}(dx)}{\mathbb{M}(dx)}$. The following result represents the starting point for the idea of importance sampling.

**Lemma 2**

*For any measurable, integrable and bounded function $\varphi : \mathcal{X} \to \mathbb{R}$, the following holds:*

$$\mathbb{E}_{\mathbb{M}}(\varphi \cdot w) = \mathbb{E}_{\mathbb{Q}}(\varphi) \cdot \mathbb{E}_{\mathbb{M}}(w) \tag{3.1}$$

**Proof.** *Note that $\mathbb{Q}(dx) = \frac{w(x)}{\mathbb{E}_{\mathbb{M}}(w)} \mathbb{M}(dx)$. Hence:*

$$\mathbb{E}_{\mathbb{Q}}(\varphi) = \int_{\mathcal{X}} \varphi(x) \mathbb{Q}(dx) = \int_{\mathcal{X}} \varphi(x) \frac{w(x)}{\mathbb{E}_{\mathbb{M}}(w)} \mathbb{M}(dx) = \frac{\mathbb{E}_{\mathbb{M}}(\varphi \cdot w)}{\mathbb{E}_{\mathbb{M}}(w)}$$

$$\blacksquare$$

Lemma 2 represents the key theoretical foundation of **importance sampling** (IS), a numerical algorithm that allows to sample from a *proposal density* to estimate moments that are computed with respect to the *target density*, by means of re-weighting the values of the target function $\varphi$.

Adopting the previous notation, the target measure is $\mathbb{Q}$, while the proposal is $\mathbb{M}$. IS requires to sample $N$ values from $\mathbb{M}$, then to find the associated *normalized*[2] weights $W(X^n)$, finally to compute a weighted average of the values taken by the function $\varphi$. The IS is implemented according to the following algorithm.

1. Sample $N$ values from the proposal measure: $X^n \sim \mathbb{M}$ for $n = 1, ..., N$.

2. Compute the associated normalized weights: $W(X^n)$ for $n = 1, ..., N$

3. Compute the estimator:

$$\hat{\varphi} = \frac{1}{N} \sum_{n=1}^{N} \varphi(X^n) W(X^n).$$

---

[2]Weights are normalized when $\mathbb{E}_{\mathbb{M}}(W) = 1$. In this case $W$ is the Radom-Nikodym derivative between $\mathbb{Q}$ and $\mathbb{M}$.

Note that $\hat{\varphi}$ is an unbiased estimator for the target of inference $\mathbb{E}_{\mathbb{Q}}(\varphi)$. In fact:

$$\mathbb{E}_{\mathbb{M}}(\hat{\varphi}) = \frac{1}{N}\sum_{n=1}^{N}\mathbb{E}_{\mathbb{M}}(\varphi \cdot W) = \mathbb{E}_{\mathbb{M}}(\varphi \cdot W) = \mathbb{E}_{\mathbb{Q}}(\varphi)$$

where the last equality follows from lemma 2 and the fact that weights are normalized to 1.

### 3.1.1.1  Auto-normalized IS

Usually, the Radom-Nikodym derivative is known up to a normalizing constant and the IS algorithm has to be described in more general terms. In the previous section the *normalized* weighting function $W(\cdot)$ was the Radom-Nikodym derivative of $\mathbb{Q}$ with respect to $\mathbb{M}$. More generally, consider the function $w(x) \propto \frac{\mathbb{Q}(dx)}{\mathbb{M}(dx)}$, denoted as *importance function*, proportional to the derivative $W(\cdot)$.

In this case, weights have to be *auto*-normalized to obtain the IS - Monte Carlo estimator. The auto-normalized IS is implemented according to the following procedure.

1. Sample $N$ values from the proposal measure: $X^n \sim \mathbb{M}$ for $n = 1, ..., N$.

2. Compute the associated *un-normalized* weights: $w(X^n)$ for $n = 1, ..., N$.

3. Normalize the weights, for $n = 1, ..., N$:

$$W^n := \frac{w(X^n)}{\sum_{m=1}^{N} w(X^m)}$$

4. Compute the estimator:

$$\hat{\varphi}_{AN} = \sum_{n=1}^{N} \varphi(X^n) W^n$$

While the auto-normalized estimator is biased (since $W^n$ involves a ratio of random variables), it is consistent (see 3.1.1.2 for details).

It is useful to interpret IS as an algorithm that allows to find an approximation for the probability measure $\mathbb{Q}$ as a weighted average of Dirac measures for the sampled values $(X^n)$: $\delta_{X^n}(dx)$ where the weights are the auto-normalized ones $(W^n)$. In particular:

$$\mathbb{Q}^N(dx) := \sum_{n=1}^{N} W^n \delta_{X^n}(dx), \quad X^n \sim \mathbb{M} \tag{3.2}$$

Furthermore, the IS estimator is the expected value of the function $\varphi$ with respect to the approximating probability measure $\mathbb{Q}^N$:

$$\mathbb{E}_{\mathbb{Q}^N}(\varphi) = \int_{\mathcal{X}} \varphi(x)\mathbb{Q}^N(dx) = \int_{\mathcal{X}} \varphi(x)\sum_{n=1}^{N} W^n \delta_{X^n}(dx) =$$

$$= \sum_{n=1}^{N} \int_{\mathcal{X}} \varphi(x)W^n \delta_{X^n}(dx) = \sum_{n=1}^{N} \varphi(X^n)W^n = \hat{\varphi}_{AN}$$

### 3.1.1.2    Convergence of the IS estimator

Consider the auto-normalized IS estimator $\hat{\varphi} = \sum_{n=1}^{N} \varphi(X^n) W^n$. We can write:

$$\hat{\varphi}_{AN} - \mathbb{E}_{\mathbb{Q}}(\varphi) = \mathbb{E}_{\mathbb{Q}^N}(\varphi) - \mathbb{E}_{\mathbb{Q}}(\varphi) = \frac{N^{-1} \sum_{n=1}^{N} w(X^n) [\varphi(X^n) - \mathbb{E}_{\mathbb{Q}}(\varphi)]}{N^{-1} \sum_{n=1}^{N} w(X^n)}$$

Let $\bar{\varphi}(X) := \varphi(X) - \mathbb{E}_{\mathbb{Q}}(\varphi)$. Applying the CLT to the numerator, assuming that $\mathbb{E}_{\mathbb{M}}(w^2 \bar{\varphi}^2) < +\infty$, we get:

$$\sqrt{N} \left\{ \frac{1}{N} \sum_{n=1}^{N} w(X^n) \bar{\varphi}(X^n) \right\} \implies \mathcal{N}\left(0, \mathbb{E}_{\mathbb{M}}(w^2 \bar{\varphi}^2)\right) \tag{3.3}$$

where $\implies$ denotes convergence in distribution. Instead, for the denominator the strong LLN implies that:

$$\frac{1}{N} \sum_{n=1}^{N} w(X^n) \to \mathbb{E}_{\mathbb{M}}(w) \quad \text{a.s.} \tag{3.4}$$

Applying Slutsky's theorem, together with (3.3) and (3.4), we obtain:

$$\sqrt{N}\left[\hat{\varphi}_{AN} - \mathbb{E}_{\mathbb{Q}}(\varphi)\right] \implies \mathcal{N}\left(0, \frac{\mathbb{E}_{\mathbb{M}}(w^2 \bar{\varphi}^2)}{[\mathbb{E}_{\mathbb{M}}(w)]^2}\right) \tag{3.5}$$

Therefore, the IS (auto-normalized) estimator for $\varphi$ is both consistent and asymptotically normal.

### 3.1.1.3    Effective Sample Size

A common measure of efficiency for IS is the *effective sample size* (ESS), defined as:

$$ESS(W^{1:N}) := \frac{1}{\sum_{n=1}^{N} (W^n)^2} = \frac{\left[\sum_{n=1}^{N} w(X^n)\right]^2}{\sum_{n=1}^{N} (w(X^n))^2}$$

Observe that the $ESS$ lies in the interval $[1, N]$. For instance, if $W^n = 1/N$, as in the case of the standard MC method, $ESS = N$.

It is possible to relate the $ESS$ to the variance of the importance function. In fact:

$$\frac{N}{ESS} = 1 + \frac{N^{-1} \sum_{n=1}^{N} (w(X^n))^2 - \left[N^{-1} \sum_{n=1}^{N} w(X^n)\right]^2}{\left[N^{-1} \sum_{n=1}^{N} w(X^n)\right]^2}$$

The second term in the numerator of the previous formula is the square of the coefficient of variation (i.e., the ratio between the variance and the squared mean) of the un-normalized weights. It is clear that a lower $ESS$ is associated with a higher variance for the weights.

## 3.1.2    Sequential Importance Sampling

When dealing with state-space models, the importance sampling algorithm has to be applied dynamically and the importance weights are updated period-by-period. To illustrate the relevance of the *sequential importance*

*sampling* (SIS) algorithm, we consider a two-period stochastic process.

Let us consider the approximation of the measure $\mathbb{Q}_0$ obtained at time 0 through IS from the measure $\mathbb{M}_0$:

$$\mathbb{Q}_0^N(dx_0) = \sum_{n=1}^{N} W_0^n \delta_{X_0^n}(dx_0), \quad \text{with } X_0^n \sim \mathbb{M}_0, \quad \text{and } W_0^n := \frac{w_0(X_0^n)}{\sum_{m=1}^{N} w_0(X_0^m)}.$$

Moreover, let $M_1(x_0, dx_1)$ be the transition kernel. We want to update, sequentially, the approximating measure $\mathbb{Q}_0$ to obtain an approximation of the measure:

$$\mathbb{Q}_1(dx_{0:1}) = \mathbb{Q}_0(dx_0)M_1(x_0, dx_1)$$

SIS works according to the following algorithm.

1. Sample $N$ values for $X_0$ from the proposal measure $\mathbb{M}_0$: $X_0^n \sim \mathbb{M}_0$ for $n = 1, ..., N$.

2. Sample $N$ values for $X_1$ from the transition kernel $M_1$: $X_1^n \sim M_1(X_0^n, dx_1)$ for $n = 1, ..., N$.

3. Compute the auto-normalized weights. In this case, they are computed taking into account only time 0 sampled observations since $X_1^n$ is sampled from the correct distribution: $W_1^n = W_0^n$.

Therefore, the particle approximation of $\mathbb{Q}_1(dx_{0:1})$ is:

$$\mathbb{Q}_1^N(dx_{0:1}) = \sum_{n=1}^{N} W_0^n \delta_{X_0^n}(dx_0)M_1(X_0^n, dx_1)$$

### 3.1.3 Sequential Importance Resampling

A second approach can be used when sampling has to be done sequentially: *sequential importance resampling* (SIR). Differently from SIS, an intermediate resampling stage takes place, in which time 0 values are sampled with replacement according to a given resampling strategy (usually, sampling indexes from a multinomial distribution with probabilities equal to the weights computed through IS at time 0).

While in the SIS all the particles (i.e., the sampled values) "survive", with the "risk" that particles associated with small weights are carried-over (in the sense that sampling in period 1 occurs from the kernel $M_1(X_0^n, dx_1)$), the same does not occur in SIR. In this second algorithm, particles with larger weights are more likely to be resampled and be used to "generate" the particles in the next period.

We describe the SIR more formally, focusing on the previous two-period case.

1. Sample $N$ values $X_0$ from the proposal measure $\mathbb{M}_0$: $X_0^n \sim \mathbb{M}_0$ for $n = 1, ..., N$.

2. Compute the weights $W_0^n$ for $n = 1, ..., N$.

3. Sample $N$ indexes $(A_1^1, ...A_1^N)$ from a multinomial distribution such that for all $j = 1, ...N$, $Pr(\{A_1^j = n\}) = W_0^n$, for all $n = 1, ...N$.

4.  Build a new time 0 sample, using the values for $X_0$ associated to the previously extracted indexes $(A_1^n)_n$:

$$(X_0^{A_1^1}, ..., X_0^{A_1^N}).$$

5.  Sample $N$ values for $X_1$ from the transition kernel $M_1$: $X_1^n \sim M_1(X_0^{A_1^n}, dx_1)$ for $n = 1, ..., N$.

Steps 3-4 constitute the actual resampling ones. At this point, let us define the new two-period sequence $\tilde{X}_{0:1}^n := (X_0^{A_1^n}, X_1^n)$. Then, the particle approximation for the joint distribution of $(X_0, X_1)$ becomes:

$$\mathbb{Q}_1^N(dx_{0:1}) = \frac{1}{N} \sum_{n=1}^{N} \delta_{\tilde{X}_{0:1}^n}(dx_{0:1})$$

Note that, after resampling occurred, each particle $\tilde{X}_{0:1}^n := (X_0^{A_1^n}, X_1^n)$ has the same probability weight.

To understand the reason of the previous statement, let us assume that both $\mathbb{Q}_0$ and $\mathbb{M}_0$ admit densities $q_0$, $m_0$ with respect to the same dominating measure $v(dx_0)$ and that the transition kernel $M_1$ also admits the density $m_1$. Consider the sequential updating for the weights:

$$w_1^n = \frac{\mathbb{Q}_1(dx_{0:1})}{\mathbb{M}_1(dx_{0:1})} \propto \frac{q_0(x_0^{A_1^n})}{Pr(A_1^n) \cdot m_0(x_0^{A_1^n})} \cdot \frac{m_1(x_1^n|x_0^{A_1^n})}{m_1(x_1^n|x_0^{A_1^n})} = \underbrace{\frac{q_0(x_0^{A_1^n})}{m_0(x_0^{A_1^n})}}_{W_0^n} \cdot \underbrace{\frac{1}{Pr(A_1^n)}}_{1/W_0^n} = 1 \tag{3.6}$$

where $\mathbb{M}_1$ denotes the probability measure for the extraction of the particle $\tilde{x}_{0:1}^n$ according to SIR. $\mathbb{M}_1$ (second equality sign in the previous formula) can be rewritten as the product between the kernel for $x_1^n$ given $x_0^{A_1^n}$ and the probability of $x_0^{A_1^n}$ itself. This last probability can also be rewritten as the product between the proposal density $m_0$ from which $X_0$ is extracted and the probability that it is sampled again when resampling occurs.

### 3.1.4  SIS vs SIR

The choice between the two sequential sampling strategies (SIS and SIR) has significant implications in terms of computational cost and variance of the importance weights. In fact, it is clear that SIR is more costly computationally since it requires an intermediate resampling step. Nonetheless, SIS suffers from the problem knonw as *curse of dimensionality*, i.e., the fact that the *ES S* collapses over time as the variance of the weights diverges.

Consider an extension of SIS to a $T$-period model and let us assume that the target and the proposal kernels admit densities, respectively, $q_t$ and $m_t$ with respect to the same dominating measures (this implies that the joint distributions[3] admit a density too). Then, weights, for every $t = 1, ..., T$, are updated according to:

$$w_t^n \propto \frac{q_t(x_{0:t}^n)}{m_t(x_{0:t}^n)} \propto \underbrace{\frac{q_{t-1}(x_{0:t-1}^n)}{m_{t-1}(x_{0:t-1}^n)}}_{\propto w_{t-1}^n} \cdot \frac{q_t(x_t|x_{t-1}^n)}{m_t(x_t|x_{t-1}^n)} \propto w_{t-1}^n \cdot \frac{q_t(x_t|x_{t-1}^n)}{m_t(x_t|x_{t-1}^n)} \tag{3.7}$$

---

[3]Let us denote the joint distributions with $q_t$ and $m_t$ too, with some abuse of notation.

Equation (3.7) suggests, intuitively, that over time new variance is added from the incremental weights (i.e., the updating factor $q_t(x_t|x_{t-1}^n)/m_t(x_t|x_{t-1}^n)$) determining the curse of dimensionality issue. Instead, when resampling takes place, since the past weights $w_{t-1}$ are reset to be equal across them all the variance of $w_t$ inherited from the past is shut-down and the only source of variability at each stage comes from the incremental weights.

## 3.2 Particle Filter

Let us consider the standard state-space model introduced previously (see 1.3). *Particle filter* (PF) is a numerical algorithm that is used to obtain approximations for the filtering - $\mathbb{P}_t(dx_t|y_{1:t})$ - and the prediction - $\mathbb{P}_t(dx_t|y_{1:t-1})$ - distributions for inference in state-space models.

In a state-space model sampling sequentially from the transition kernels for the states is not enough to obtain good approximations since the observation sample ($y_{1:T}$) contains information about the underlying states through the likelihood function $f_t(y_t|x_t)$. Observations constitute signals for the model's states.

Therefore, the conditional distribution of the states, given the observed data - $\mathbb{P}_t(dx_{1:t}|y_{1:t})$ - changes over time as new data points become available. The PF algorithm allows to incorporate sequentially the new data to obtain new approximations for this distribution (and for the filtering and prediction ones).

In general, at each step of the algorithm, states are sampled sequentially from the proposal measure, call it $\mathbb{M}_t$, and importance auto-normalized weights are computed as the Radom-Nikodym derivative of the target $\mathbb{P}_t$ with respect to the proposal $\mathbb{M}_t$. Moreover, the Markov properties of the sequence of the states allows to update sequentially the importance weights.

We will analyse three different types of particle filtering procedures: *bootstrap*, *guided* and *auxiliary particle filters*, that differ between them with respect to their scope and efficiency.

### 3.2.1 Degeneracy of the SIS in Particle Filter

Usually, PF requires a resampling step at each stage of the algorithm. Recall that, in general, resampling determines a trade-off between the increase in the variance at the resampling stage and a decrease in the variance when future states are sampled from the transition kernel.

"Dead" particles (i.e., those with small weights) are likely to be removed when resampling takes place and past weights get "reset" (usually, they are set to be equal to $1/N$). Otherwise, the *curse of dimensionality* problem will emerge and the variance of the weights will diverge over time as the variance of past weights increases as new updates occur period-by-period. Next, we show an example of a PF where SIS is used: note that the

*ESS* drops dramatically after few periods, meaning that the variance of the importance weights diverges. This motivates the use of a SIR structure for the PF algorithm.

Lastly, it is now common practice to use a mixed approach with respect to resampling (recall that resampling has an additional computational cost). Generally, resampling is done *adaptively*, when some condition is met. A standard criterion that is used (and that we adopt in our implementations of the PF) is to resample when the *ESS* drops below some threshold $ESS_{min} \in [1, N]$:

$$ESS(W_{t-1}^{1:N}) < ESS_{min} \tag{3.8}$$

### 3.2.2   Implementation

Consider again the random walk plus noise model of section 2.0.1,the challenge here is to estimate the filtered states using a Sequential Importance Sampling algorithm. The main idea of the SIS applied to this univariate linear gaussian model is described in the following algorithm. We indicate with *n* the sample size of time observations and with *N* the generated sample size for each step of the Sequenial Monte Carlo.

**Algorithm**  *SIS filter for Random Walk plus Noise Model*

- *Let $\{(x_0, w_0)^{(i)}\}_{i=1}^{N}$ summarize $p(x_0|y_0)$ such that, for example, $E(g(x_0)|y_0) \approx \sum_{i=1}^{N} w_0^{(i)} g(x_0^{(i)})$. In particular, initialize $(x_0^{(1)}, ..., x_0^{(N)})$ form $N(m_0, C_0)$ and set $w_0^{(i)} = N^{-1} \ \forall \ i = 1, ..., N$.*

- *For $t = 1, ..., n$:*

    1. *Draw $x_t^{(i)} \sim N(x_{t-1}^{(i)}, \tau^2) \ i = 1, ..., N$ such that $\{(x_t, w_{t-1})^{(i)}\}_{i=1}^{N}$ summarizes $p(x_t|y_{t-1})$*

    2. *Set $w_t^{(i)} = w_{t-1}^{(i)} f_N(y_t; x_t^{(i)}, \sigma^2) \ i = 1, ..., N$ such that $\{(x_t, w_t)^{(i)}\}_{i=1}^{N}$ summarizes $p(x_t|y_t)$*

    3. *Set $p(x_t|y_t) = \sum_{i=1}^{N} w_t^{(i)} \delta_{x_t^{(i)}}$*

Our `SISfun` function implemented in R replicate this steps.

---

```
SISfun(data,N,m0,C0,tau,sigma)
```

---

**Arguments**

`data`   the observed process. It has to be a vector or a univariate time series.

`N`   number of particles generated at each step

`m0`   central value of the normal prior state distribution

`C0`   variance of the normal prior state distribution

tau   the standard deviation $\tau$ in state equation

sigma   the standard deviation $\sigma$ in observation equation

```r
SISfun<-function(data,N,m0,C0,tau,sigma){
  xs<-NULL
  ws<-NULL
  ess<-NULL
  x  = rnorm(N,m0,sqrt(C0))
  w  = rep(1/N,N)
  for(t in 1:length(data)){
    x   = rnorm(N,x,tau)
    w   = w*dnorm(data[t],x,sigma)
    xs = rbind(xs,x)
    ws = rbind(ws,w)


    wnorm= w/sum(w)
    ESS  = 1/sum(wnorm^2)


    ess =rbind(ess,ESS)
  }


  return(list(xs=xs,ws=ws,ess=ess))
}
```

We have already discussed the reasons why the SIS algorithm does not provide a good strategy in the filtering problem. We provide a graphical intuition of what happens when we use such filtering strategy on a simulated dataset. We decide to set $N = 1000$, $m_0 = 0$, $C_0 = 100$ and $\tau = \sigma = 1$. The following two plots show a clear degeneration of the effective sample size and bad fit of filtered states with respect to the true values.
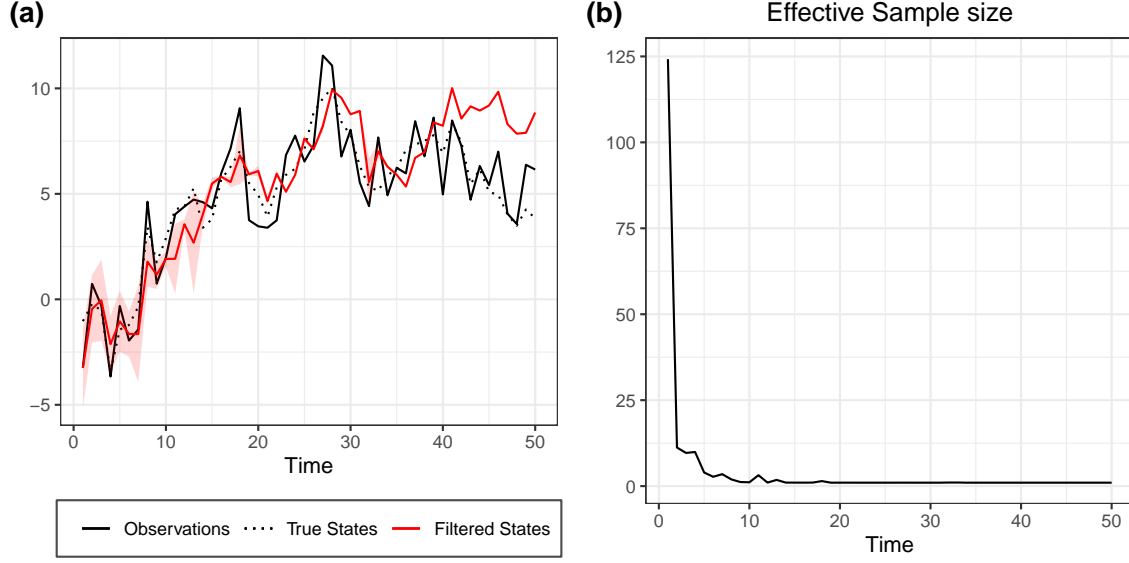
**(a)**

**(b)**                Effective Sample size



Figure 3.1: a) SIS Filtered States with credible interval (in red). b) Effective sample size.

### 3.2.3   Bootstrap Particle Filter

The bootstrap particle filter (BPF) is the easiest form of an adaptive PF algorithm. In fact, future states are sampled from the *correct* transition kernel and the weights are updated sequentially using the likelihood $f_t(y_t|x_t)$.

We summarize the procedure with the following scheme.

1. **Inital stage:** For $n = 1, ..., N$, at time 0 sample: $X_0^n \sim \mathbb{P}_0(dx_0)$ and set the un-normalized weights $w_0^n = 1$. Then, the normalized weights are: $W_0^n = \frac{1}{N}$.

2. **For every** $t = 1, ...T$:

   (a) **Resample** if $ESS\left(W_{t-1}^{1:N}\right) < ESS_{min}$:[4]

      i. Multinomial sampling for the indexes $(A_t^n)_n$ with probabilities given by $(W_{t-1}^n)_n$.

---

[4]It is indifferent to implement this resampling step at the beginning or at the end of each iteration (as we do in our codes) as long as the initial stage $t = 0$ generates weights that are constant and equal to $1/N$. In fact, in this case, resampling will never take place at the beginning of the first iteration since $ESS\left(W_0^n = 1/N\right) = N$ that is larger than or equal to $ESS_{min}$. However, when we describe the algorithm, we chose to leave this resampling step at the beginning of each iteration. In fact, when considering the guided or auxiliary PF, we can, more generally, sample the initial values (time $t = 0$) for the state from a proposal distribution different from the target one. In this case, the weights at $t = 0$ might differ from $1/N$, hence resampling might take place already at the beginning of the first iteration.

ii. Update weights as: $\hat{w}_{t-1}^n = 1$ for $n = 1, ..., N$.

**Otherwise,**

i. Set the indexes: $A_t^n = n$ for $n = 1, ..., N$.

ii. Set the weights: $\hat{w}_{t-1}^n = w_{t-1}^n$ for $n = 1, ..., N$.

(b) Sample the future states from the transition kernel: $X_t^n \sim P_t(X_{t-1}^{A_t^n}, dx_t)$ for $n = 1, ..., N$.

(c) Update the un-normalized weights through the likelihood function for $n = 1, ..., N$.:

$$w_t^n = \hat{w}_{t-1}^n \cdot f_t(y_t|X_t^n).$$

(d) Normalize the weights for $n = 1, ..., N$.: $W_t^n := \frac{w_t^n}{\sum_{m=1}^N w_t^m}$.

Therefore, at the initial step the pre-sample period states $x_0^n$ are extracted and every sampled state is assigned an equal weight since there is no corresponding observation $y_0$ that gives additional information on the likelihood of that extraction.

Resampling does never take place in $t = 1$[5] and the state in $t = 1$ is sampled from the correct transition kernel $P_1(x_0^n, dx_1)$. Now, the time 0 weights are updated incorporating the information from the data point $y_1$ in a very intuitive way: more *likely* states (given $y_1$) are given higher weights: $w_1^n = f_1(y_1|x_1^n)$. This weights are used to approximate the time 1 filtering distribution.

At a subsequent stage, the *ESS* criterion should be checked and, in case it is satisfied, resampling takes place and time 1 weights are reset to be equal to $1/N$.

The key characteristic of the PF is the fact that the importance weights are updated sequentially, according to the "information" provided by the observed data (i.e., the sequence $y_{1:T}$). Recall that time $t$ weight is the Radom-Nikodym derivative of the target with respect to the proposal distribution. In the BPF, the time $t$ target is the measure $\mathbb{P}_t(dx_{0:t}|y_{1:t})$, while the proposal, denoted generically by $\mathbb{M}_t$, is $\mathbb{M}_t(dx_{0:t}|y_{1:t}) = \mathbb{M}_{t-1}(dx_{0:t-1}|y_{1:t-1}) \cdot P_t(x_{t-1}, dx_t)$. Hence:

$$
\begin{aligned}
w_t &\propto \frac{\mathbb{P}_t(dx_{0:t}|y_{1:t})}{\mathbb{M}_t(dx_{0:t}|y_{1:t})} \propto \frac{\mathbb{P}_{t-1}(dx_{0:t-1}|y_{1:t-1}) \cdot P_t(x_{t-1}, dx_t) \cdot f(y_t|x_t)}{\mathbb{M}_{t-1}(dx_{0:t-1}|y_{1:t-1}) \cdot P_t(x_{t-1}, dx_t)} = \\
&= \underbrace{\frac{\mathbb{P}_{t-1}(dx_{0:t-1}|y_{1:t-1})}{\mathbb{M}_{t-1}(dx_{0:t-1}|y_{1:t-1})}}_{\hat{w}_{t-1}} \cdot f(y_t|x_t) = \hat{w}_{t-1} \cdot f(y_t|x_t)
\end{aligned}
\tag{3.9}
$$

Finally, the BPF is able to generate the two key objects for inference in state-space models:

---

[5]Since $ESS(W_0^n = 1/N) = N \geq ESS_{min}$.

- the predictive distribution:

$$\mathbb{P}_t^N(dx_t|y_{1:t-1}) = \frac{1}{\sum_{n=1}^N \hat{w}_t^n} \sum_{n=1}^N \hat{w}_t^n \delta_{X_t^n}(dx_t) =$$

$$= \begin{cases} \frac{1}{N} \sum_{n=1}^N \delta_{X_t^n}(dx_t) & \text{if resampling occurs} \\ \frac{1}{\sum_{n=1}^N w_{t-1}^n} \sum_{n=1}^N w_{t-1}^n \delta_{X_t^n}(dx_t) & \text{otherwise} \end{cases} \quad , \qquad (3.10)$$

- the filtering distribution:

$$\mathbb{P}_t^N(dx_t|y_{1:t}) = \sum_{n=1}^N W_t^n \delta_{X_t^n}(dx_t) \qquad (3.11)$$

## 3.2.4  Implementation

In this section, Bootstrap Particle Filter will be used to estimate filtered states of the Random Walk plus Noise introduced in section 2.0.1. The overall strategy replicate the SIS filter with the addition of a ESS-based resampling step that applies when the effective sample size is smaller than a predetermined threshold opportunely chosen (in our example we decide to follow a common rule of thumb consisting in setting the threshold at $N/2$). The steps are presented in the following algorithm.

**Algorithm**  *BPF for Random Walk plus Noise Model*

- *Let $\{(x_0, w_0)^{(i)}\}_{i=1}^N$ summarize $p(x_0|y_0)$ such that, for example, $E(g(x_0)|y_0) \approx \sum_{i=1}^N w_0^{(i)} g(x_0^{(i)})$. In particular, initialize $(x_0^{(1)}, ..., x_0^{(N)})$ form $N(m_0, C_0)$ and set $w_0^{(i)} = N^{-1} \; \forall \; i = 1, ..., N$.*

- *For $t = 1, ..., n$:*

  1. *Draw $x_t^{(i)} \sim N(x_{t-1}^{(i)}, \tau^2) \; i = 1, ..., N$ such that $\{(x_t, w_{t-1})^{(i)}\}_{i=1}^N$ summarizes $p(x_t|y_{1:t-1})$*

  2. *Set $w_t^{(i)} = w_{t-1}^{(i)} f_N(y_t; x_t^{(i)}, \sigma^2) \; i = 1, ..., N$ such that $\{(x_t, w_t)^{(i)}\}_{i=1}^N$ summarizes $p(x_t|y_{1:t})$*

  3. *Normalize the weights: $w_t^{(i)} = \frac{\tilde{w}_t^{(i)}}{\sum_{j=1}^N (\tilde{w}_t^{(j)})}$*

  4. *Compute $ESS = \left( \sum_{i=1}^N (w_t^{(i)})^2 \right)^{-1}$*

  5. *if $ESS < N/2$ then*

     (a) *Draw a sample of size N, $(x_t^{(1)}, ..., x_t^{(N)})$, from the discrete distribution $P(x_t = x_t^{(i)}) = w_t^{(i)}, \; i = 1, ..., N$*

     (b) *Reset the weights: $w_t^{(i)} = N^{-1}, i = 1, ..., N$.*

  6. *Set $p(x_t|y_{1:t}) = \sum_{i=1}^N w_t^{(i)} \delta_{x_t^{(i)}}$*

These steps are resumed in our `PFfun` function.

---

```
PFfun(data,N,m0,C0,tau,sigma,r)
```

---

**Arguments**

`data`   the observed process. It has to be a vector or a univariate time series.

`N`   number of particles generated at each step

`m0`   central value of the normal prior state distribution

`C0`   variance of the normal prior state distribution

`tau`   the standard deviation $\tau$ in state equation

`sigma`   the standard deviation $\sigma$ in observation equation

`r`   if present the threshold is set equal to $N/r$ otherwise, if missing, the threshold is set equal to $N/2$

```r
PFfun<-function(data,N,m0,C0,tau,sigma,r){

  if(missing(r)){r=2}else{}

  xs<-NULL

  ws<-NULL

  ess<-NULL

  x  = rnorm(N,m0,sqrt(C0))

  w  = rep(1/N,N)


  for(t in 1:length(data)){


    x<-rnorm(N,x,tau)

    w1<-w*dnorm(data[t],x,sigma)


    w = w1/sum(w1)

    ESS  = 1/sum(w^2)


    if(ESS<(N/r)){

      index<-sample(N,size=N,replace=T,prob=w)

      x<-x[index]

      w<-rep(1/N,N)
```

```
    }else{}


    xs = rbind(xs,x)

    ws = rbind(ws,w)

    ess =rbind(ess,ESS)

  }

  return(list(xs=xs,ws=ws,ess=ess))

}
```

The estimated states of the Boostrap Particle Filter togheter with the effective sample size are shown in Figure 3.2. We decide to set $N = 1000$, $m_0 = 0$, $C_0 = 100$ and $\tau = \sigma = 1$. Notice how the resampling step allows the effective sample size not to drop, improving results.
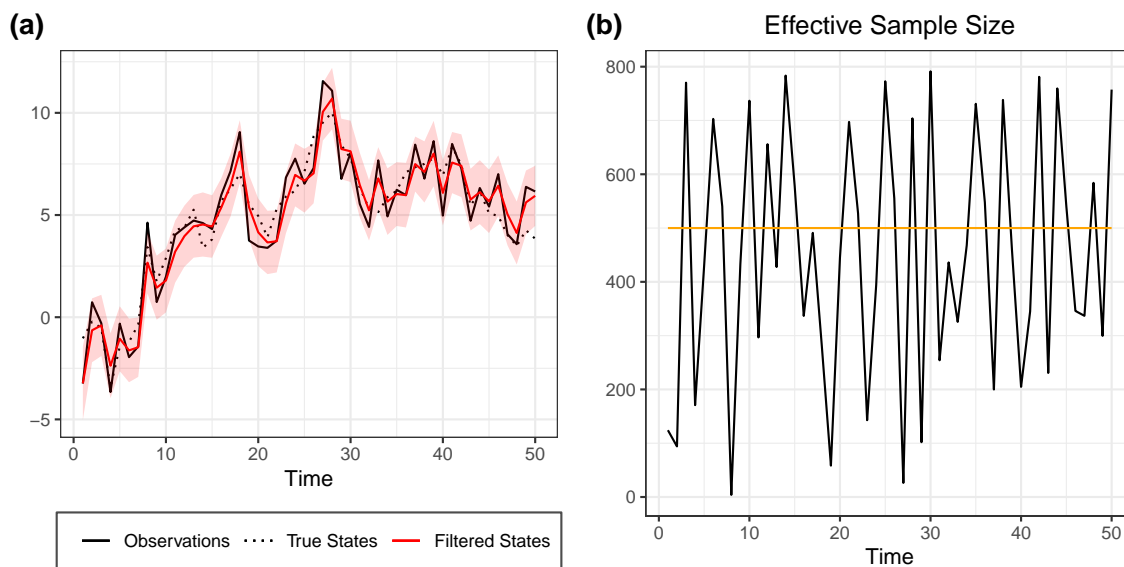


Figure 3.2: a) PF Filtered States with credible interval (in red). b) Effective sample size (in black) with threshold (in yellow).

Since the Random Walk plus Noise model allows for closed form solutions, we want to compare the results of Boostrap Particle Filter(BPF) with Kalman Filter(KF). As we can see from figure 3.3, when the number of particles generated at any interaction increases the results for both the estimated mean and the variance tend to converge [[SPIEGARE PERCHE']]. Moreover, comparing the Root Mean Square Errors of the filtered states

with respect to the true state values, when the sample size increases the BPF decreases and, for large N, it reaches the accuracy of the Kalman Filter.

Table 3.1: Root Mean Square Errors

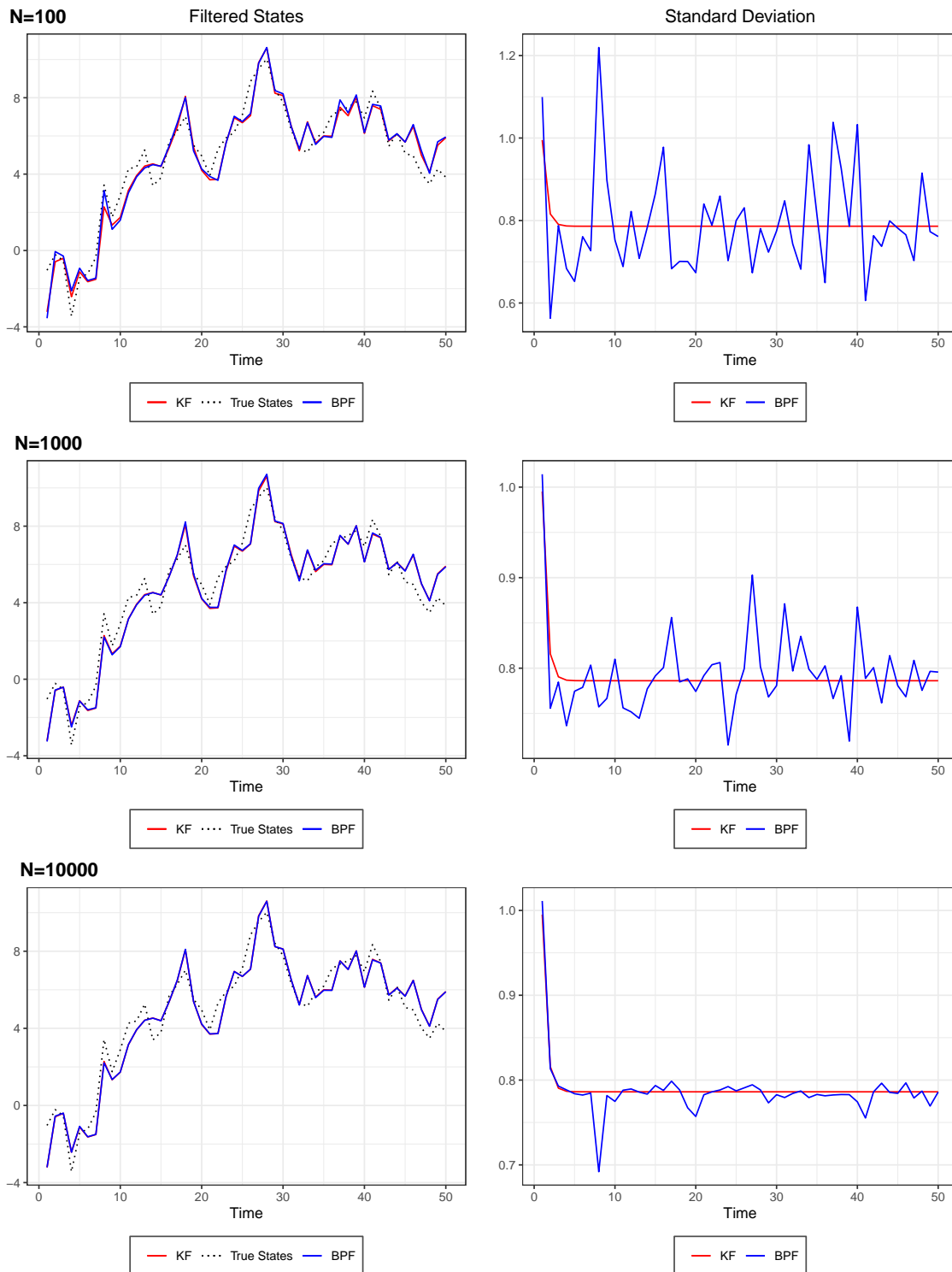| N | Threshold | KF | BPF |
|---|---|---|---|
| 100 | 0.5 | 0.879 | 0.916 |
| 1000 | 0.5 | 0.879 | 0.882 |
| 10000 | 0.5 | 0.879 | 0.885 |

Figure 3.3: Comparison Bootstrap Particle Filter(BPF) and Kalman Filter (KF) for increasing number of generated particles (N)

### 3.2.5 Guided Particle Filter

It is not always possible to sample sequentially from the correct transition kernel. Moreover, even if it were possible, there exist a proposal transition kernel that makes the algorithm more efficient. This motivates the *guided particle filter* (GPF), that can be interpreted as a more general version of the BPF. In fact, with the GPF it is possible, at each stage, to sample new states from a transition kernel that differs from the correct one. Let $P_t(x_{t-1}, dx_t)$ be the correct kernel and consider a kernel $M_t(x_{t-1}, dx_t)$ defined on the same measurable space of $P_t$. Moreover, let us assume that that $P_t$ is absolutely continuous with respect to $M_t$[6] (i.e., $P_t \ll M_t$). If sampling occurs sequentially from this kernel, the way in which weights are updated should differ from the BPF. Consider equation (3.9) and let us reformulate it for the GPF case. Here, the proposal distribution is not $\mathbb{M}_t(dx_{0:t}|y_{1:t}) = \mathbb{M}_{t-1}(dx_{0:t-1}|y_{1:t-1}) \cdot P_t(x_{t-1}, dx_t)$ anymore, but becomes $\mathbb{M}_t(dx_{0:t}|y_{1:t}) = \mathbb{M}_{t-1}(dx_{0:t-1}|y_{1:t-1}) \cdot M_t(x_{t-1}, dx_t)$. Hence:

$$w_t \propto \frac{\mathbb{P}_t(dx_{0:t}|y_{1:t})}{\mathbb{M}_t(dx_{0:t}|y_{1:t})} \propto \frac{\mathbb{P}_{t-1}(dx_{0:t-1}|y_{1:t-1}) \cdot P_t(x_{t-1}, dx_t) \cdot f_t(y_t|x_t)}{\mathbb{M}_{t-1}(dx_{0:t-1}|y_{1:t-1}) \cdot M_t(x_{t-1}, dx_t)} =$$
$$= \underbrace{\frac{\mathbb{P}_{t-1}(dx_{0:t-1}|y_{0:t-1})}{\mathbb{M}_{t-1}(dx_{0:t-1}|y_{1:t-1})}}_{\hat{w}_{t-1}} \cdot \frac{P_t(x_{t-1}, dx_t) \cdot f_t(y_t|x_t)}{M_t(x_{t-1}, dx_t)} = \hat{w}_{t-1} \cdot \underbrace{\frac{P_t(x_{t-1}, dx_t) \cdot f_t(y_t|x_t)}{M_t(x_{t-1}, dx_t)}}_{\text{updating factor}} \tag{3.12}$$

Note that the updating factor is more complex that the one of the BPF: in addition to the likelihood function $f_t(y_t|x_t)$, the fact that sampling occurs from a kernel different from the correct ones requires the additional term $P_t(x_{t-1}, dx_t)/M_t(x_{t-1}, dx_t)$.

We are now ready to establish, informally, the optimality result about the transition kernel. Let us denote by $G_t = [P_t(x_{t-1}, dx_t) \cdot f_t(y_t|x_t)dy_t]/M_t(x_{t-1}, dx_t)$ the *incremental weights* (i.e., the updating factor) and by $M_t^*(x_{t-1}, dx_t)$ the optimal kernel. It can be proved[7] that the optimal kernel, i.e., the one that minimizes the variance of the incremental weights $G_t$ (and of the time $t$ weights themselves), is:

$$M_t^*(x_{t-1}, dx_t) = \frac{1}{\int_{\mathcal{X}} P_t(x_{t-1}, dx_t) \cdot f_t(y_t|x_t)} P_t(x_{t-1}, dx_t) \cdot f_t(y_t|x_t) \tag{3.13}$$

Note that $M_t^*$ is the conditional distribution of $x_t$ given $x_{t-1}$ and $y_t$.[8] The intuition for this result is apparent when considering equation (3.12): if $M_t = M_t^*$, the updating factor collapses to $\int_{\mathcal{X}} P_t(x_{t-1}, dx_t) \cdot f_t(y_t|x_t)$ and

---

[6]This condition is stronger than what would be needed for the existence of the importance weights in GPF, i.e., that $P_t(x_{t-1}, dx_t) \cdot f_t(y_t|x_t) \ll M_t(x_{t-1}, dx_t)$.

[7]For a formal proof see Chopin and Papaspiliopoulos (2020), th. 10.1 p. 142.

[8]In fact, assuming that the $P_t$ admits a density $p_t$, applying Bayes rule, we have that $m_t(x_t|x_{t-1}, y_t) \propto p_t(x_t|x_{t-1}) \cdot f(y_t|x_t)$.

information from the observed data are incorporated efficiently.

As a matter of fact, it is usually impossible to sample from the optimal kernel and, in practice, it is replaced by its linear Gaussian approximation.

The GPF can be resumed by the following steps.

1. **Inital stage:** For $n = 1, ..., N$, at time 0 sample: $X_0^n \sim \mathbb{M}_0(dx_0)$ and set the un-normalized weights:

$$w_0^n = \frac{\mathbb{P}_0(dx_0)}{\mathbb{M}_0(dx_0)}.$$

   Then, the normalized weights are: $W_0^n := \frac{w_0^n}{\sum_{m=1}^{N} w_0^m}$.

2. **For every** $t = 1, ...T$**:**

   (a) **Resample** if $ESS(W_{t-1}^{1:N}) < ESS_{min}$:

      i.  Multinomial sampling for the indexes $(A_t^n)_n$ with probabilities given by $(W_{t-1}^n)_n$.

      ii. Update weights as: $\hat{w}_{t-1}^n = 1$ for $n = 1, ..., N$.

      **Otherwise,**

      i.  Set the indexes: $A_t^n = n$ for $n = 1, ..., N$

      ii. Set the weights: $\hat{w}_{t-1}^n = w_{t-1}$ for $n = 1, ..., N$.

   (b) Sample the future states from the transition kernel: $X_t^n \sim M_t(X_{t-1}^{A_t^n}, dx_t)$ for $n = 1, ..., N$.

   (c) Update the un-normalized weights, for $n = 1, ..., N$:

$$w_t^n = \hat{w}_{t-1}^n \cdot \frac{P_t(X_{t-1}^{A_t^n}, dx_t) \cdot f_t(y_t|X_t^n)}{M_t(X_{t-1}^{A_t^n}, dx_t)}.$$

   (d) Normalize the weights, for $n = 1, ..., N$: $W_t^n := \frac{w_t^n}{\sum_{m=1}^{N} w_t^m}$.

Note that $\mathbb{M}_0(dx_0)$ is the initial sampling distribution, that could differ from the correct one $\mathbb{P}_0(dx_0)$.

To conclude, one of the issues related to the BPF is the fact that new states in $t$ are sampled ignoring their likelihood given the future observation $y_t$. Hence, extractions from the "correct" transition kernel may be associated to low weights (small value for the likelihood). Instead, the GPF allows to solve for this problem, defining a proposal kernel that depends on the likelihood itself. Therefore, the extraction of future states already incorporates the information given by the data resulting in a more efficient procedure.

### 3.2.6 Implementation

The Bootstrap Particle Filter Approach for the Random Walk plus Noise Model described in Section 2.0.1 can be improved accounting for the observations in the importance transition density and it consists of generating $x_t$ from its conditional distribution given $x_{t-1}$ and $y_t$. In the Normal model we are considering, the optimal proposal will be a Normal density as well with mean and variance given by

$$\mu_{opt} = E(x_t|x_{t-1}, y_t) = x_{t-1} + \frac{\tau^2}{\tau^2 + \sigma^2}(y_t - x_{t-1})$$

$$\sigma^2_{opt} = V(x_t|x_{t-1}, y_t) = \frac{\tau^2 \sigma^2}{\tau^2 + \sigma^2}$$

On the other hand, the incremental weights, using this importance transition density, are proportional to the conditional density of $y_t$ given $x_{t-1} = x_{t-1}^{(i)}$ , i.e $N(x_{t-1}^{(i)}, \tau^2 + \sigma^2)$, evaluated at $y_t$. In other words the algorithm implemented in R is:

**Algorithm** *GPF for Random Walk plus Noise Model*

- *Let $\{(x_0, w_0)^{(i)}\}_{i=1}^{N}$ summarize $p(x_0|y_0)$ such that, for example, $E(g(x_0)|y_0) \approx \sum_{i=1}^{N} w_0^{(i)} g(x_0^{(i)})$. In particular, initialize $(x_0^{(1)}, ..., x_0^{(N)})$ from $N(m_0, C_0)$ and set $w_0^{(i)} = N^{-1} \ \forall \ i = 1, ..., N$.*

- *Compute $\sigma^2_{opt}$*

- *For $t = 1, ..., n$:*

    1. *Compute $\mu_{opt}$*

    2. *Draw $x_t^{(i)} \sim N(\mu_{opt}, \sigma^2_{opt})$ $i = 1, ..., N$ such that $\{(x_t, w_{t-1})^{(i)}\}_{i=1}^{N}$ summarizes $p(x_t|y_{1:t-1})$*

    3. *Set $w_t^{(i)} = w_{t-1}^{(i)} f_N(y_t; x_t^{(i)}, \sigma^2 + \tau^2)$ $i = 1, ..., N$ such that $\{(x_t, w_t)^{(i)}\}_{i=1}^{N}$ summarizes $p(x_t|y_{1:t})$*

    4. *Normalize the weights: $w_t^{(i)} = \frac{\tilde{w}_t^{(i)}}{\sum_{j=1}^{N}(\tilde{w}_t^{(j)})}$*

    5. *Compute $ESS = \left( \sum_{i=1}^{N} (w_t^{(i)})^2 \right)^{-1}$*

    6. *if $ESS < N/2$ then*

        (a) *Draw a sample of size N, $(x_t^{(1)}, ..., x_t^{(N)})$, from the discrete distribution $P(x_t = x_t^{(i)}) = w_t^{(i)}$, $i = 1, ..., N$*

        (b) *Reset the weights: $w_t^{(i)} = N^{-1}$, $i = 1, ..., N$.*

    7. *Set $p(x_t|y_{1:t}) = \sum_{i=1}^{N} w_t^{(i)} \delta_{x_t^{(i)}}$*

The GPFfun function resume this passages.

---

```
GPFfun(data,N,m0,C0,tau,sigma,r)
```

---

**Arguments**

data   the observed process. It has to be a vector or a univariate time series.

N   number of particles generated at each step

m0   central value of the normal prior state distribution

C0   variance of the normal prior state distribution

tau   the standard deviation $\tau$ in state equation

sigma   the standard deviation $\sigma$ in observation equation

r   if present the threshold is set equal to $N/r$ otherwise, if missing, the threshold is set equal to $N/2$

```r
GPFfun<-function(data,N,m0,C0,tau,sigma,r){

  if(missing(r)){r=2}else{}

  xs<-NULL

  ws<-NULL

  ess<-NULL

  x   = rnorm(N,m0,sqrt(C0))

  importancesd<-sqrt(tau - tau^2 /(tau + sigma))

  predsd <- sqrt(sigma+tau)

  w   = rep(1/N,N)


  for(t in 1:length(data)){


    means<-x+(tau/(tau+sigma))*(data[t]-x)

    x<-rnorm(N,means,importancesd)

    w1<-w*dnorm(data[t],x,predsd)


    w = w1/sum(w1)

    ESS   = 1/sum(w^2)


    if(ESS<(N/r)){
```

```
        index<-sample(N,size=N,replace=T,prob=w)

        x<-x[index]

        w<-rep(1/N,N)

    }else{}


    xs = rbind(xs,x)

    ws = rbind(ws,w)

    ess =rbind(ess,ESS)

  }

  return(list(xs=xs,ws=ws,ess=ess))

}
```
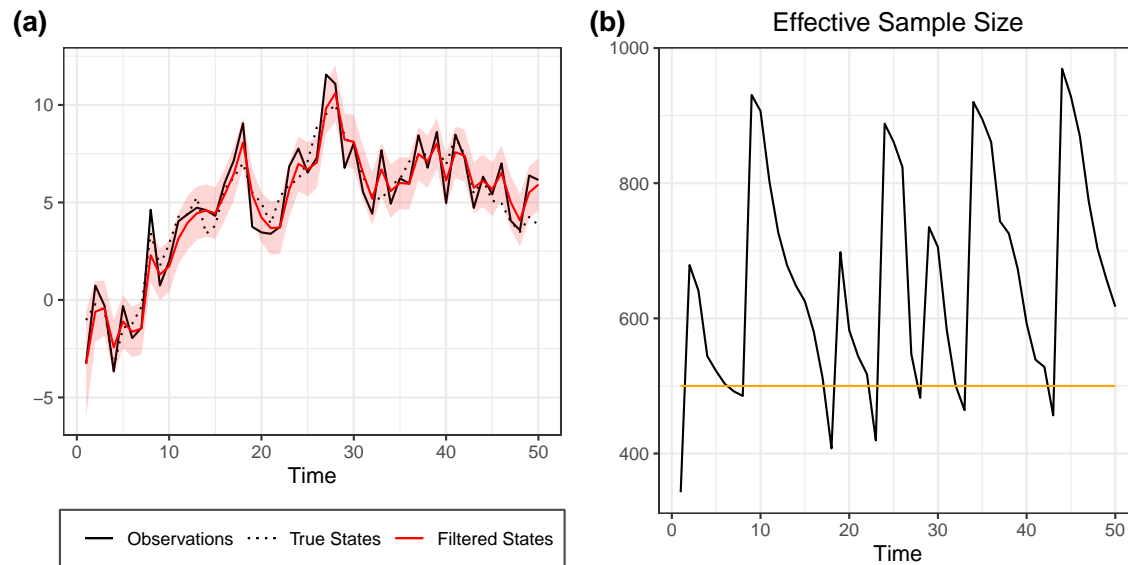


Figure 3.4: a) GPF Filtered States with credible interval (in red). b) Effective sample size (in black) with threshold (in yellow).

Let's provide directly a brief comparison between the Bootstrap Particle Filter (BPF) and the Guided Particle Filter (GPF). As we can see from the Figure 3.5, the Guided Particle Filter provides point estimates that are slightly better with respect to the ones of the BPF, and this is confirmed by the Table showing the RMSE. Moreover, the variance is lower, suggesting for higher precision.

Table 3.2: Root Mean Square Errors

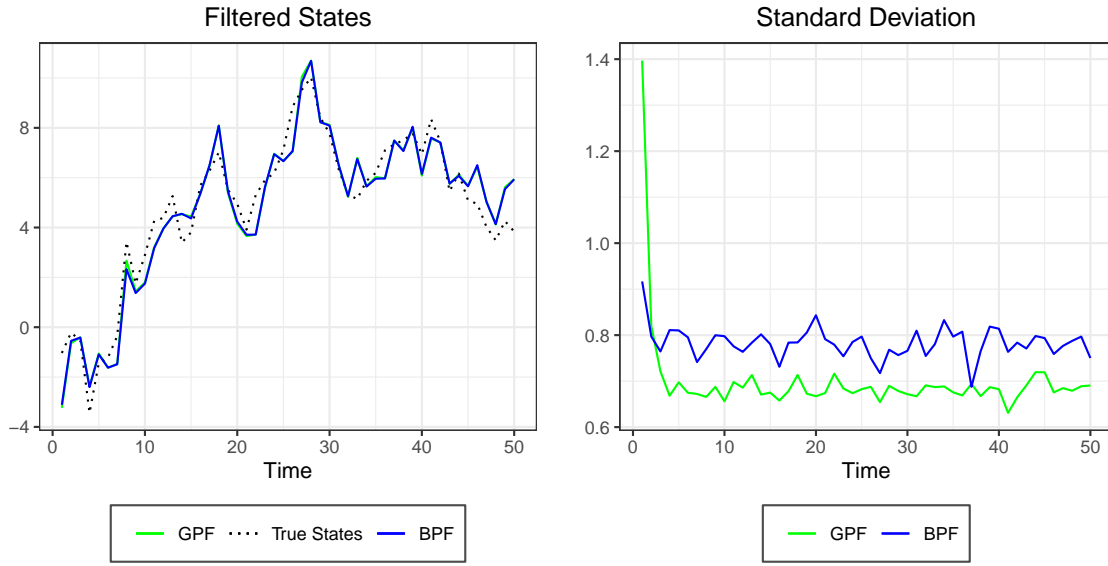| N | Threshold | BPF | GPF |
|---|---|---|---|
| 1000 | 0.50 | 0.882 | 0.874 |
| 1000 | 0.25 | 0.889 | 0.874 |
| 1000 | 0.10 | 0.885 | 0.879 |



Figure 3.5: Comparison Bootstrap Particle Filter(BPF) and Guided Particle Filter (GPF), number of generated particles N=1000

### 3.2.7   Auxiliary Particle Filter

The *auxiliary particle filter* (APF) constitutes a further extension of the BPF. The GPF allowed to sample from a transition kernel different from the correct ones. The APF, instead, allows to extract the ancestor variables from an arbitrary distribution at the resampling step.

Let $\eta_t : \mathcal{X} \to \mathbb{R}_+$ be a non-negative, real-valued positive function, called *auxiliary function*. At time $t$, when the resampling stage occurs, the multinomial distribution for the indexes to be extracted can use probabilities that differ from the weights in $t-1$, $W_{t-1}^n$. The new weights, called *auxiliary weights*, are computed as a

transformation of the original ones, denoted as *inferential weights*, through the auxiliary function:

$$\tilde{W}_t^n = \frac{W_t^n \cdot \eta_t(X_t^n)}{\sum_{m=1}^N W_t^m \cdot \eta_t(X_t^n)} \tag{3.14}$$

Note that the computation of the auxiliary weights is done from the auto-normalized inferential ones. Additionally, note that imposing $\eta_t(x_t) = 1$ we recover the GPF and the BPF as special cases of the APF. Clearly, inferential weights are updated by incorporating the fact that resampling occurs according to different weights (the auxiliary ones):

$$w_t^n = \frac{W_{t-1}^{A_t^n}}{\tilde{W}_{t-1}^{A_t^n}} G_t \tag{3.15}$$

where $G_t$ is the incremental weight defined in the section on GPF.

To understand the logic of this sequential weight updating, consider (3.12). In particular, suppose that multinomial resampling takes place at every stage and let $\tilde{w}_{t-1} := w_{t-1} \cdot \eta_{t-1}(x_{t-1})$. Then:

$$\begin{aligned}
w_t &\propto \frac{\mathbb{P}_t(dx_{0:t}|y_{1:t})}{\mathbb{M}_t(dx_{0:t}|y_{1:t})} \propto \frac{\mathbb{P}_{t-1}(dx_{0:t-1}|y_{0:t-1})}{\mathbb{M}_{t-1}(dx_{0:t-1}|y_{1:t-1}) \cdot \tilde{w}_{t-1}} \cdot \frac{P_t(x_{t-1}, dx_t) \cdot f_t(y_t|x_t)}{M_t(x_{t-1}, dx_t)} \\
&= \underbrace{\frac{\mathbb{P}_{t-1}(dx_{0:t-1}|y_{0:t-1})}{\mathbb{M}_{t-1}(dx_{0:t-1}|y_{1:t-1})}}_{w_{t-1}} \cdot \frac{1}{\tilde{w}_{t-1}} \cdot \frac{P_t(x_{t-1}, dx_t) \cdot f_t(y_t|x_t)}{M_t(x_{t-1}, dx_t)} \\
&= \frac{w_{t-1}}{\tilde{w}_{t-1}} \cdot \frac{P_t(x_{t-1}, dx_t) \cdot f_t(y_t|x_t)}{M_t(x_{t-1}, dx_t)}
\end{aligned} \tag{3.16}$$

It is possible to derive an optimality result for the auxiliary functions[9]. In the special case in which the transition kernel used for sampling corresponds with the optimal one $M_t^*$, the optimal auxiliary function (i.e., the auxiliary function that minimizes the variance of the inferential weights) becomes:

$$\eta_{t-1}^*(x_{t-1}) = \int_{\mathcal{X}} P_t(x_{t-1}, dx_t) f_t(y_t|x_t) \tag{3.17}$$

and is called *perfectly adapted* auxiliary function. In fact, if $M_t = M_t^*$, then, expression (3.16) becomes:

$$w_t \propto \frac{w_{t-1}}{\tilde{w}_{t-1}} \cdot \frac{P_t(x_{t-1}, dx_t) \cdot f_t(y_t|x_t)}{M_t^*(x_{t-1}, dx_t)} = \frac{1}{\eta_{t-1}(x_{t-1})} \cdot \int_{\mathcal{X}} P_t(x_{t-1}, dx_t) f_t(y_t|x_t)$$

From the previous equation, it is clear that if $\eta_t = \eta_t^*$, the inferential weights are constant and their variance is zero.

We can summarize the APF algorithm.

1. **Inital stage:**

---

[9]Details in Chopin and Papaspiliopoulos (2020) th 10.2, p. 148

(a) For $n = 1, ..., N$, at time 0 sample: $X_0^n \sim \mathbb{M}_0(dx_0)$ and set the un-normalized inferential weights:

$$w_0^n = \frac{\mathbb{P}_0(dx_0)}{\mathbb{M}_0(dx_0)}.$$

Then, the normalized inferential weights are: $W_0^n := \frac{w_0^n}{\sum_{m=1}^N w_0^m}$.

(b) Compute the un-normalized auxiliary weights:

$$\tilde{w}_0^n = w_0^n \cdot \eta_0(X_0^n)$$

Then the normalized auxiliary weights are: $\tilde{W}_0^n := \frac{\tilde{w}_0^n}{\sum_{m=1}^N \tilde{w}_0^m}$.

2. **For every** $t = 1, ...T$**:**

   (a) **Resample** if $ESS(W_{t-1}^{1:N}) < ESS_{min}$:

      i. Multinomial sampling for the indexes $(A_t^n)_n$ with probabilities given by $(\tilde{W}_{t-1}^n)_n$.

      ii. Update weights as: $\hat{w}_{t-1}^n = \frac{W_{t-1}^{A_t^n}}{\tilde{W}_{t-1}^{A_t^n}}$ for $n = 1, ..., N$.

   **Otherwise,**

      i. Set the indexes: $A_t^n = n$ for $n = 1, ..., N$.

      ii. Set the weights: $\hat{w}_{t-1}^n = w_{t-1}$ for $n = 1, ..., N$.

   (b) Sample the future states from the transition kernel: $X_t^n \sim M_t(X_{t-1}^{A_t^n}, dx_t)$ for $n = 1, ..., N$.

   (c) Update the un-normalized inferential weights, for $n = 1, ..., N$:

   $$w_t^n = \hat{w}_{t-1}^n \cdot \frac{P_t(X_{t-1}^{A_t^n}, dx_t) \cdot f_t(y_t|X_t^n)}{M_t(X_{t-1}^{A_t^n}, dx_t)}.$$

   (d) Normalize the inferential weights, for $n = 1, ..., N$: $W_t^n := \frac{w_t^n}{\sum_{m=1}^N w_t^m}$.

   (e) Compute the un-normalized auxiliary weights, for $n = 1, ..., N$:

   $$\tilde{w}_t^n = w_t^n \cdot \eta_t(X_t^n)$$

   (f) Normalize the auxiliary weights, for $n = 1, ..., N$: $\tilde{W}_t^n := \frac{\tilde{w}_t^n}{\sum_{m=1}^N \tilde{w}_t^m}$.[10]

However, it is worth noting that the optimality results both for the kernel in the GPF and of the auxiliary in the APF, has two main weaknesses:

---

[10]It is worth mentioning that the original APF included a final resampling step at the end of each iteration. However, our formulation is more efficient since having two resampling steps might introduce additional Monte Carlo variance. See Johansen and Evers (2007), p. 120

- it is not clear that what is optimal at time $t$ remains such at future stages. In other words, it is not truly clear how the minimization of the variance of the inferential weights at each stage affects the efficiency of the PF estimators;

- both the choice of $M_t$ and of $\eta_t$ affect the way in which weights are computed and, indirectly, the decision to resample in the future. It is difficult to take also this indirect effect into account when evaluating the overall efficiency of the algorithm.

### 3.2.8   Implementation

For illustration purposes, we are going implement an auxiliary particle filter for the linear Gaussian model with auxiliary function $g(x_{t-1}) = E(x_t | x_{t-1}) = x_{t-1}$.

**Algorithm**  *APF for Random Walk plus Noise Model*

- *Let $\{(x_0, w_0)^{(i)}\}_{i=1}^N$ summarize $p(x_0|y_0)$ such that, for example, $E(g(x_0)|y_0) \approx \sum_{i=1}^N w_0^{(i)} g(x_0^{(i)})$. In particular, initialize $(x_0^{(1)}, ..., x_0^{(N)})$ from $N(m_0, C_0)$ and set $w_0^{(i)} = N^{-1} \; \forall \; i = 1, ..., N$.*

- *For $t = 1, ..., n$:*

    1. *For $k = 1, ..., N$:*

        (a) *Draw $I_k$ with $P(I_k = i) \propto w_{t-1}^{(i)} f(y_t | g(x_{t-1}^{(i)}))$*

        (b) *Draw $x_t^{(k)} \sim N(x_{t-1}^{(I_k)}, \tau^2)$*

        (c) *Set $\tilde{w}_t^{(k)} = \frac{f_N(y_t | x_t^{(k)})}{f_N(y_t | g(x_{t-1}^{(I_k)}))}$*

    2. *Normalize the weights: $w_t^{(i)} = \frac{\tilde{w}_t^{(i)}}{\sum_{j=1}^N (\tilde{w}_t^{(j)})}$*

    3. *Compute $ESS = \left( \sum_{i=1}^N (w_t^{(i)})^2 \right)^{-1}$*

    4. *if $ESS < N/2$ then*

        (a) *Draw a sample of size N, $(x_t^{(1)}, ..., x_t^{(N)})$, from the discrete distribution $P(x_t = x_t^{(i)}) = w_t^{(i)}$,  $i = 1, ..., N$*

        (b) *Reset the weights: $w_t^{(i)} = N^{-1}$, $i = 1, ..., N$.*

    5. *Set $p(x_t | y_{1:t}) = \sum_{i=1}^N w_t^{(i)} \delta_{x_t^{(i)}}$*

The `APFfun` function resume this passages.

---

```
APFfun(data,N,m0,C0,tau,sigma,r)
```

---

**Arguments**

`data`  the observed process. It has to be a vector or a univariate time series.

`N`  number of particles generated at each step

`m0`  central value of the normal prior state distribution

`C0`  variance of the normal prior state distribution

`tau`  the standard deviation $\tau$ in state equation

`sigma`  the standard deviation $\sigma$ in observation equation

`r`  if present the threshold is set equal to $N/r$ otherwise, if missing, the threshold is set equal to $N/2$

```r
APFfun<-function(data,N,m0,C0,tau,sigma,r){

  if(missing(r)){r=2}else{}

  xs<-NULL

  ws<-NULL

  ess<-NULL

  x  = rnorm(N,m0,sqrt(C0))

  w  = rep(1/N,N)


  for(t in 1:length(data)){


    weight = w*dnorm(data[t],x,sigma)

    k    = sample(1:N,size=N,replace=TRUE,prob=weight)

    x1   = rnorm(N,x[k],tau)

    lw   = dnorm(data[t],x1,sigma,log=TRUE)-dnorm(data[t],x[k],sigma,log=TRUE)

    w    = exp(lw)

    w    = w/sum(w)

    ESS  = 1/sum(w^2)


    if(ESS<(N/r)){
```

```
      index<-sample(N,size=N,replace=T,prob=w)

      x1<-x1[index]

      w<-rep(1/N,N)

   }else{}


   x <- x1

   xs = rbind(xs,x)

   ws = rbind(ws,w)

   ess =rbind(ess,ESS)


  }
  return(list(xs=xs,ws=ws,ess=ess))
}
```

**(a)**



**(b)** Effective Sample Size
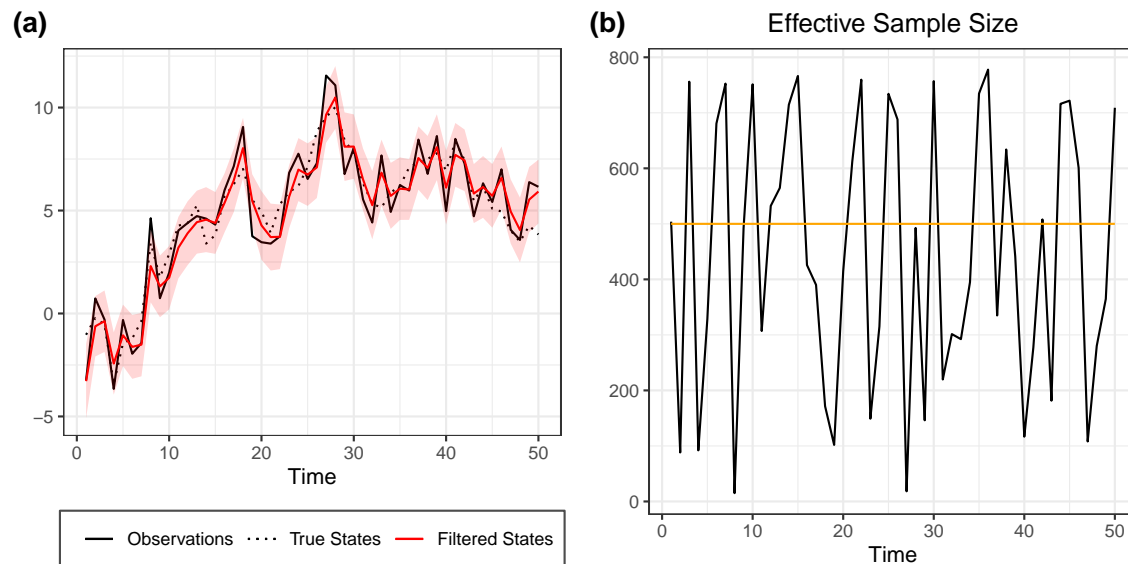
Figure 3.6: a) APF Filtered States with credible interval (in red). b) Effective sample size (in black) with threshold (in yellow).

Let's compare the Auxiliary Particle Filter (APF) and the Bootstrap Particle Filter (BPF). From Figure 3.7 it is difficult to say which of the two is better and the tables does not help much since the APF apparently outperforms the BPF in two cases over three. For this reason we can conclude that for this model the Auxiliary

Particle Filtering strategy does not provide any serious improvement to a the basic one.
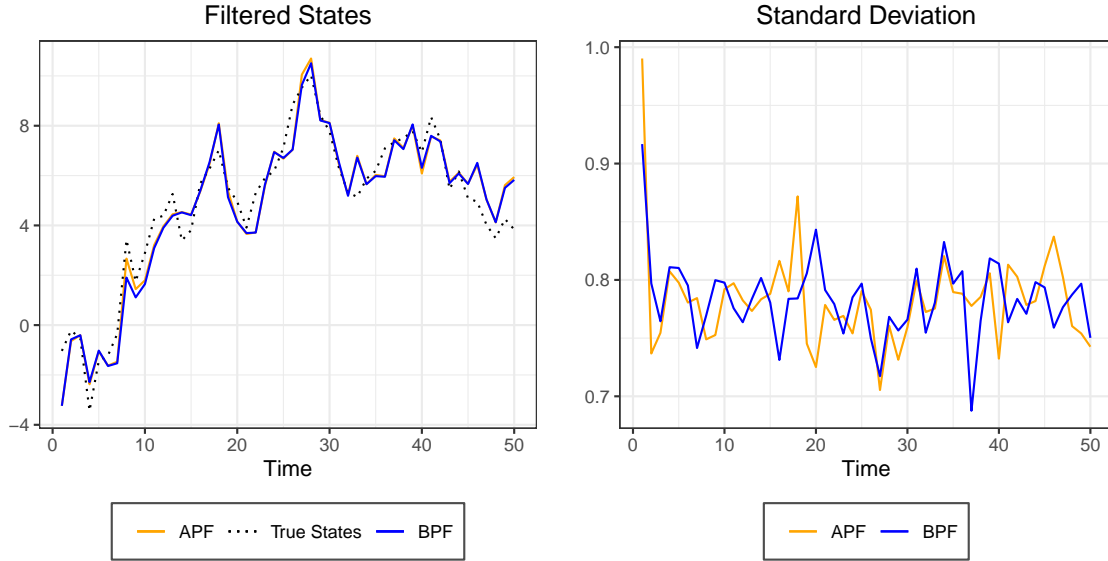


Figure 3.7: Comparison Bootstrap Particle Filter(BPF) and Guided Particle Filter (GPF), number of generated particles N=1000

Table 3.3: Root Mean Square Errors

| N | Threshold | BPF | APF |
|------|-----------|-------|-------|
| 1000 | 0.50 | 0.882 | 0.899 |
| 1000 | 0.25 | 0.889 | 0.883 |
| 1000 | 0.10 | 0.885 | 0.877 |

We also implement the auxiliary particle filter with optimal transition kernel. Therfore the algorithm is similiar to the one discussed above with the difference that:

**Algorithm** *APF with optimal transition kernel for Random Walk plus Noise Model*

- *Let $\{(x_0, w_0)^{(i)}\}_{i=1}^N$ summarizes $p(x_0|y_0)$ such that, for example, $E(g(x_0)|y_0) \approx \sum_{i=1}^N w_0^{(i)} g(x_0^{(i)})$. In particular, initialize $(x_0^{(1)}, ..., x_0^{(N)})$ from $N(m_0, C_0)$ and set $w_0^{(i)} = N^{-1} \ \forall \ i = 1, ..., N.$*

- *Compute $\sigma_{opt}^2$*

- *For $t = 1, ..., n$:*

1. *Compute* $ESS = \left( \sum_{i=1}^{N} (w_t^{(i)})^2 \right)^{-1}$

2. *if* $ESS < N/2$ *then*

    (a) *Draw* $I_k$ *with* $P(I_k = i) \propto w_{t-1}^{(i)} f_N(y_t | g(x_{t-1}^{(i)}), \sigma^2 + \tau^2)$

    (b) *Compute* $\mu_{opt} = \mu(x_{t-1}^{(I_k)})$

    (c) *Draw* $x_t^{(k)} \sim N(\mu_{opt}, \sigma_{opt}^2)$

    (d) *Set* $\tilde{w}_t^{(i)} = N^{-1}$ *for* $i = 1, ..., N$

3. *otherwise*

    (a) *Compute* $\mu_{opt} = \mu(x_{t-1})$

    (b) *Draw* $x_t^{(i)} \sim N(\mu_{opt}, \sigma_{opt}^2)$ *for* $i = 1, ... N$

    (c) *Set* $\tilde{w}_t^{(i)} = w_{t-1}^{(i)} f_N(y_t; x_t^{(i)}, \sigma^2 + \tau^2)$ *for* $i = 1, ..., N$

4. *Normalize the weights:* $w_t^{(i)} = \frac{\tilde{w}_t^{(i)}}{\sum_{j=1}^{N} (\tilde{w}_t^{(j)})}$

```r
APFoptfun<-function(data,N,m0,C0,tau,sigma,r){
  if(missing(r)){r=2}else{}
  xs<-NULL
  ws<-NULL
  ess<-NULL
  x   = rnorm(N,m0,sqrt(C0))
  importancesd<-sqrt(tau - tau^2 /(tau + sigma))
  predsd <- sqrt(sigma+tau)
  w   = rep(1/N,N)


  for(t in 1:length(data)){
    ESS  = 1/sum(w^2)


    if(ESS<(N/r)){
    weight = w*dnorm(data[t],x,predsd)
    k    = sample(1:N,size=N,replace=TRUE,prob=weight)
    means<-x[k]+(tau/(tau+sigma))*(data[t]-x[k])
```

```r
  x1   = rnorm(N,means,importancesd)
  w   = rep(1/N,N)
  }else{
  weight = rep(1/N,N)
  k    = sample(1:N,size=N,replace=FALSE,prob=weight)
  means<-x[k]+(tau/(tau+sigma))*(data[t]-x[k])
  x1   = rnorm(N,means,importancesd)
  w    <-  w*dnorm(data[t],x1,predsd)
  }


  w   = w/sum(w)
  x <- x1



  xs = rbind(xs,x)
  ws = rbind(ws,w)
  ess =rbind(ess,ESS)


 }
 return(list(xs=xs,ws=ws,ess=ess))
}
```
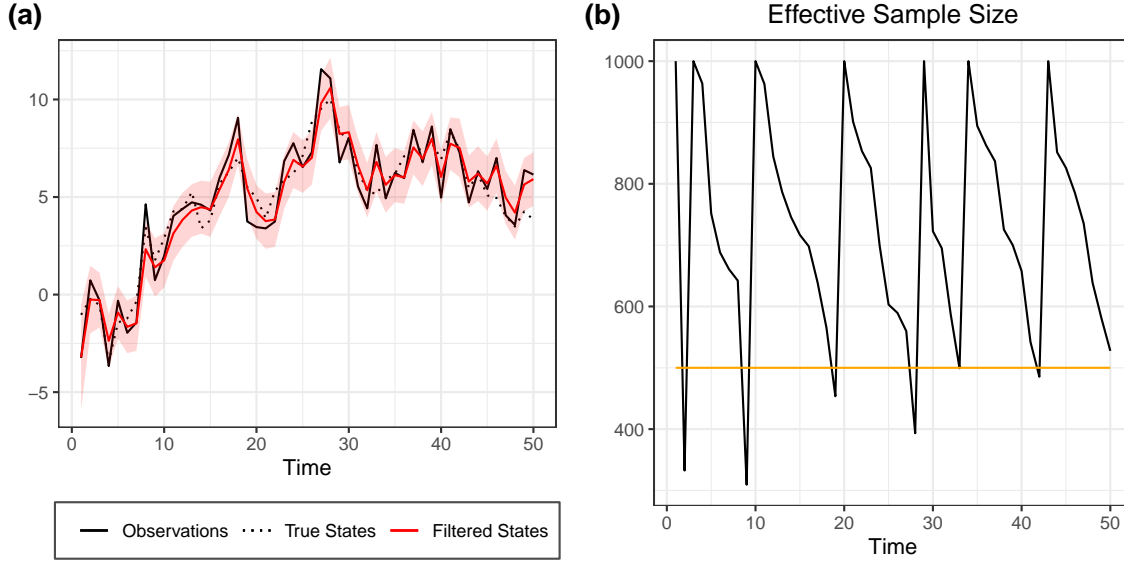
Figure 3.8: a) APF Filtered States with credible interval (in red). b) Effective sample size (in black) with threshold (in yellow).

## 3.3 Liu and West Filter

Let us consider a more general state-space model, where the state vector includes a time-constant parameter vector $\psi \in \Psi$, where $\Psi$ is the parameter space. Since we can interpret the parameter as a state with the law of motion $\psi_t = \psi_{t-1} = \psi$, then it is possible to adopt a PF algorithm to estimate $\psi$.

However, being $\psi$ constant over time, it is meaningless to sample its values sequentially: the first extraction of $\psi$ at the initial stage 0 (i.e., $\psi_0^n$) generates a constant path of particles for the parameter ($\psi_t^n = \psi_0^n$). [11]

Therefore, Liu and West (2001) proposed a modified particle filter, called *Liu and West filter* (LWF) that allows to resample the parameter over time from a continuous distribution. In this way, at every time, the support of $\psi$ is not limited to the initially sampled $N$ values.

Here, we describe the LWF that makes use of the normal distribution to sample sequentially the parameter. Moreover, consider the simpler version of the bootstrap filter.[12]

Let the transition kernel and the likelihood depend on the parameter $\psi$ (i.e., $P_t(x_{t-1}, dx_t; \psi)$ and $f_t(y_t|x_t; \psi)$)

---

[11]To be more precise, at the resampling step, also $\psi^n$ is resampled, but the possible values that it may take are the $N$ ones obtained at the initial time 0 extraction.

[12]Clearly, the LWF can be also used within the more general frameworks of the GPF and the APF. For instance, in our implementation with the random walk model of section 2.0.1, we use an auxiliary particle LWF.

and let $\pi(\cdot)$ be the prior distribution for the parameter $\psi$.

The LWF can be described by the following algorithm.

1.  **Inital stage:** For $n = 1, ..., N$, at time 0 sample: $X_0^n \sim \mathbb{P}_0(dx_0)$ and $\psi_0^n \sim \pi(\psi_0)$.

    Then, set the un-normalized weights $w_0^n = 1$.

    Hence, the normalized weights are: $W_0^n = \frac{1}{N}$.

2.  **For every** $t = 1, ...T$**:**

    (a)  **Resample** if $ESS(W_{t-1}^{1:N}) < ESS_{min}$:

        i.  Multinomial sampling for the indexes $(A_t^n)_n$ with probabilities given by $(W_{t-1}^n)_n$.

        ii.  Update weights as: $\hat{w}_{t-1}^n = 1$ for $n = 1, ..., N$.

        **Otherwise,**

        i.  Set the indexes: $A_t^n = n$ for $n = 1, ..., N$

        ii.  Set the weights: $\hat{w}_{t-1}^n = w_{t-1}$ for $n = 1, ..., N$.

    (b)  **Extracting new parameter values:**

        i.  Compute the weighted average and the variance for the parameters, respectively: $\bar{\psi} = \sum_{n=1}^N W_{t-1}^n \psi^n$, $\Omega = \sum_{n=1}^N W_{t-1}^n (\psi^n - \bar{\psi})^2$.

        ii.  Compute: $m^n = a \cdot \psi^n + (1 - a) \cdot \bar{\psi}$ for $n = 1, ..., N$.

        iii.  Draw new parameters: $\psi^n \sim \mathcal{N}\left(m^{A_t^n}, h^2 \cdot \Omega\right)$ for $n = 1, ..., N$.

    (c)  Sample future states from the transition kernel: $X_t^n \sim P_t(X_{t-1}^{A_t^n}, dx_t; \psi^n)$ for $n = 1, ..., N$.

    (d)  Update the un-normalized weights through the likelihood function, for $n = 1, ..., N$:

$$w_t^n = \hat{w}_{t-1}^n \cdot f_t(y_t | X_t^n; \psi^n).$$

    (e)  Normalize the weights, for $n = 1, ..., N$: $W_t^n := \frac{w_t^n}{\sum_{m=1}^N w_t^m}$.

At the initial step, $N$ states and $N$ parameter values are sampled independently, respectively, from $\mathbb{P}_0$ and $\pi$ and the particle weights are set to be constant, as usual.

Then, at each iteration (time $t$), the decision to resample is done according to the *ESS* criterion and indexes are extracted from a multinomial distribution. However, in the LWF both previous periods states and parameters are resampled.

Meanwhile, to extract the next period states and parameters it is necessary, firstly, to sample the new $N$ parameter values. Let $\bar{\psi}$ be the weighted average of the parameter values and $\Omega$ be their variance (the weights used to compute this mean and variance are the previous period inferential ones, i.e. $W^n_{t-1}$).

The algorithm suggests to sample new values for the parameters from a continuous distribution, i.e., a Normal[13] centered at the (resampled) values $m^{A^n_t}$ with variance $h^2 \cdot \Omega$ where $m^n$ is a convex combination of the sample mean $\bar{\psi}$ and the actual extraction of $\psi^n$ with coefficient $a \in (0,1)$ and $h$ is a scalar such that $a^2 + h^2 = 1$. While it would be more intuitively immediate to sample new parameters from a Normal density centered at the previously sampled values (i.e., $\psi^n$), this would increase the variance of $\psi$ over time.

In fact, let $\pi^N_{t-1}(\psi) = \sum_{n=1}^N \hat{W}^{A^n_t}_{t-1} \cdot \mathcal{N}(\psi^{A^n_t}, \Omega)$[14] be the empirical distribution of the parameters. From the law of iterated expectation and total variance, we obtain:[15]

$$
\begin{aligned}
\mathbb{E}_{\pi^N_{t-1}}(\psi) &= \mathbb{E}\big[\mathbb{E}(\psi|A^n_t)\big] = \mathbb{E}\big[\psi^{A^n_t}\big] = \bar{\psi} \\
Var_{\pi^N_{t-1}}(\psi) &= Var\big[\mathbb{E}(\psi|A^n_t)\big] + \mathbb{E}\big[Var(\psi|A^n_t)\big] = Var\big[\psi^{A^n_t}\big] + \mathbb{E}\big[\Omega\big] = 2 \cdot \Omega
\end{aligned}
$$

Hence, while the mean is preserved, the variance increases at each iteration. Instead, sampling from the distribution proposed by Liu and West $\mathcal{N}\big(m^{A^n_t}, h^2 \cdot \Omega\big)$ preserves both the mean and the variance of the parameters over time.

Let $\tilde{\pi}^N_{t-1}(\psi) = \sum_{n=1}^N \hat{W}^{A^n_t}_{t-1} \cdot \mathcal{N}\big(m^{A^n_t}, h^2 \cdot \Omega\big)$. Hence:

$$
\begin{aligned}
\mathbb{E}_{\tilde{\pi}^N_{t-1}}(\psi) &= \mathbb{E}\big[\mathbb{E}(\psi|A^n_t)\big] = \mathbb{E}\big[m^{A^n_t}\big] = \mathbb{E}\big[a \cdot \psi^{A^n_t} + (1-a) \cdot \bar{\psi}\big] = \bar{\psi} \\
Var_{\tilde{\pi}^N_{t-1}}(\psi) &= Var\big[\mathbb{E}(\psi|A^n_t)\big] + \mathbb{E}\big[Var(\psi|A^n_t)\big] = Var\big[m^{A^n_t}\big] + h^2 \cdot \mathbb{E}\big[\Omega\big] = \underbrace{(a^2 + h^2)}_{=1} \cdot \Omega = \Omega
\end{aligned}
$$

Finally, after sampling the new $N$ parameter values, conditional on these values, new states are also sampled from the transition kernel: $X^n_t \sim P_t(X^{A^n_t}_{t-1}, dx_t; \psi^n)$. Lastly, weights are updated through the incremental weights.

To conclude, it is worth noting that the LWF produces, together with the usual filtering and prediction distributions, a posterior distribution for the parameter:

$$
\pi^N_t(\psi) = \pi^N(\psi|y_{1:t}) = \sum_{n=1}^N W^n_t \delta_{\psi^n}(\psi) \tag{3.18}
$$

---

[13]More generally, distributions whose support coincides with the relevant parameter space.

[14]Big hat-weights $\hat{W}^{A^n_t}_{t-1}$ are the normalized weights after the resampling stage, equal to $1/N$ if resampling takes place, $W^n_{t-1}$ otherwise.

[15]For completeness, we specify that the first expected value in the law of iterated expectations and total variances is with respect to the distribution of the indexes and the second one with respect to each of the Normal distributions centered at $\psi^{A^n_t}$.

## 3.3.1   Implementation

Consider the linear Gaussian example of section 2.0.1, but this time with unknown variances $\tau^2$ and $\sigma^2$. Thus, let $\psi = (\sigma^2, \tau^2)$ be the unknown parameter vector and assign a gamma prior for its components,

$$\sigma^2 \sim G(\alpha_v, \beta_v)$$
$$\tau^2 \sim G(\alpha_w, \beta_w)$$

Alternatively, assign them a uniform prior if we have no knowledge of the hyperparameters. Note that in this model we sample from a Gamma distribution (instead of the Normal one, as in the previous description of the LWF) since the parameters of interest are variances, that can take only positive values. Next, we descrive the algorithm.

**Algorithm**  *LWF for Random Walk plus Noise Model*

- *Initialize $(x_0^{(1)}, ..., x_0^{(N)})$ from $N(m_0, C_0)$, $(\sigma^{2(1)}, ..., \sigma^{2(N)})$ from $G(\alpha_v, \beta_v)$ and $(\tau^{2(1)}, ..., \tau^{2(N)})$ from $G(\alpha_w, \beta_w)$.  Set $w_0^{(i)} = N^{-1} \ \forall \ i = 1, ..., N$.  Therefore $\psi^{(i)} = (\sigma^{2(i)}, \tau^{2(i)})$, and $\hat{\pi}_0 = p(x_0|y_0) = \sum_{i=1}^{N} w_0^{(i)} \delta_{(x_0^{(i)}, \psi^{(i)})}$*

- *For $t = 1, ..., n$:.*

    1. *Compute*

$$\overline{\sigma^2} = E_{\hat{\pi}_{t-1}}(\sigma^2)$$
$$\overline{\tau^2} = E_{\hat{\pi}_{t-1}}(\tau^2)$$
$$\Sigma_v = V_{\hat{\pi}_{t-1}}(\sigma^2)$$
$$\Sigma_w = V_{\hat{\pi}_{t-1}}(\tau^2)$$

*then set*

$$m_v^{(i)} = a\sigma^{2\,(i)} + (1-a)\overline{\sigma^2}$$

$$s_v^{2\,(i)} = (1-a^2)\Sigma_{\sigma^2}\alpha_v^{(i)} \qquad\qquad = \frac{(m_v^{(i)})^2}{s_v^{2\,(i)}}$$

$$\beta_v^{(i)} = \frac{(m_v^{(i)})}{s_v^{2\,(i)}}$$

$$m_w^{(i)} = a\tau^{2\,(i)} + (1-a)\overline{\tau^2}$$

$$s_w^{2\,(i)} = (1-a^2)\Sigma_{\tau^2}$$

$$\alpha_w^{(i)} = \frac{(m_w^{(i)})^2}{s_w^{2\,(i)}}$$

$$\beta_w^{(i)} = \frac{(m_w^{(i)})}{s_w^{2\,(i)}}$$

2. *For $k = 1, ..., N$:*

   - *Draw $I_k$, with $P(I_k = i) \propto w_{t-1}^{(i)} f_N(y_t | g(x_{t-1}^{(i)}), m_v)$*

   - *Draw $\sigma^{2\,(k)}$ from $G(\alpha_v^{(I_k)}, \beta_v^{(I_k)})$*

   - *Draw $\tau^{2\,(k)}$ from $G(\alpha_w^{(I_k)}, \beta_w^{(I_k)})$*

   - *Draw $x_t^{(k)}$ from $N(x_{t-1}^{(I_k)}, \tau^{2\,(k)})$*

   - *Set $\tilde{w}_t^{(k)} = \frac{f_N(y_t | x_t^{(k)}, \sigma^{2\,(k)})}{f_N(y_t | g(x_{t-1}^{(I_k)}, m_v^{(I_k)}))}$*

3. *Compute $ESS = \left( \sum_{i=1}^{N} (w_t^{(i)})^2 \right)^{-1}$*

4. *if $ESS < N/2$ then*

   (a) *Draw a sample of size N, $(x_t^{(1)}, ..., x_t^{(N)})$, from the discrete distribution $P(x_t = x_t^{(i)}) = w_t^{(i)}$, $i = 1, ..., N$*

   (b) *Reset the weights: $w_t^{(i)} = N^{-1}$, $i = 1, ..., N$.*

5. *Set $\hat{\pi}_t = p(x_t | y_{1:t}) = \sum_{i=1}^{N} w_t^{(i)} \delta_{(x_t^{(i)}, \psi^{(i)})}$*

Our `LWfun` function goes through the illustrated steps.

```
LWfun(data,N,m0,C0,alphav,betav,alphaw,betaw,delta,unif,r)
```

---

**Arguments**

data   the observed process. It has to be a vector or a univariate time series.

N   number of particles generated at each step

m0   central value of the normal prior state distribution

C0   variance of the normal prior state distribution

alphav, betav   Gamma prior hyperparameters on $\sigma^2$

alphaw,betaw   Gamma prior hyperparameters on $\tau^2$

delta   hyperparameter delta value

unif   if True then it sets a Uniform $(0, 10)$ prior on $\sigma^2$ and $\tau^2$

r   if present the threshold is set equal to $N/r$ otherwise, if missing, the threshold is set equal to $N/2$

```r
LWfun<-function(data,N,m0,C0,alphav,betav,alphaw,betaw,delta,unif,r){
  if(missing(r)){r=2}else{}
  xs     = rnorm(N,m0,sqrt(C0))
  if(unif==T){
  pars   = cbind(runif(N,0,10),runif(N,0,10))}else{}
  pars   = cbind(rgamma(N,shape=alphav,scale=betav),rgamma(N,shape=alphaw,scale=betaw))
  a      = (3*delta-1)/(2*delta)
  h2     = 1-a^2
  parss  = array(0,c(N,2,n))
  xss    = NULL
  ws     = NULL
  ess    = NULL
  w      = rep(1/N,N)
  for (t in 1:length(data)){
    meanV = weighted.mean(pars[,1],w)
    varV  = weighted.mean((pars[,1]-meanV)^2,w)
    meanW = weighted.mean(pars[,2],w)
    varW  = weighted.mean((pars[,2]-meanW)^2,w)
```

```
  muV = a*pars[,1]+(1-a)*meanV

  sigma2V = (1-a^2)*varV

  alphaV = muV^2/sigma2V

  betaV = muV/sigma2V


  muW = a*pars[,2]+(1-a)*meanW

  sigma2W = (1-a^2)*varW

  alphaW = muW^2/sigma2W

  betaW = muW/sigma2W


  weight      = w*dnorm(data[t],xs,sqrt(muV))

  k           = sample(1:N,size=N,replace=T,prob=weight)


  pars[,1]<-rgamma(N,shape=alphaV[k],rate=betaV[k])

  pars[,2]<-rgamma(N,shape=alphaW[k],rate=betaW[k])


  xsprevious<-xs[k]

  xs = rnorm(N,xs[k],sqrt(pars[,2]))


  w           = exp(dnorm( data[t],xs,sqrt(pars[,1]),log=T)-

                      dnorm( data[t],xsprevious,sqrt(muV[k]),log=T))

  w           = w/sum(w)

  ESS         = 1/sum(w^2)


  if(ESS<(N/r)){

    index<-sample(N,size=N,replace=T,prob=w)

    xs<-xs[index]

    pars<-pars[index,]

    w<-rep(1/N,N)

  }else{

    xs<-xs

    pars<-pars
```

```
    }


    xss          = rbind(xss,xs)

    parss[,,t]  = pars

    ws           = rbind(ws,w)

    ess          = rbind(ess,ESS)

  }

  return(list(xss=xss,parss=parss,ws=ws,ess=ess))

}
```

We provide an example of Liu and West filter fixing $\delta = 0.7$ and drawing $\alpha_v$, $\beta_v$, $\alpha_w$ and $\beta_w$ from a Uniform $U(0, 10)$. The results are shown in the following figure.
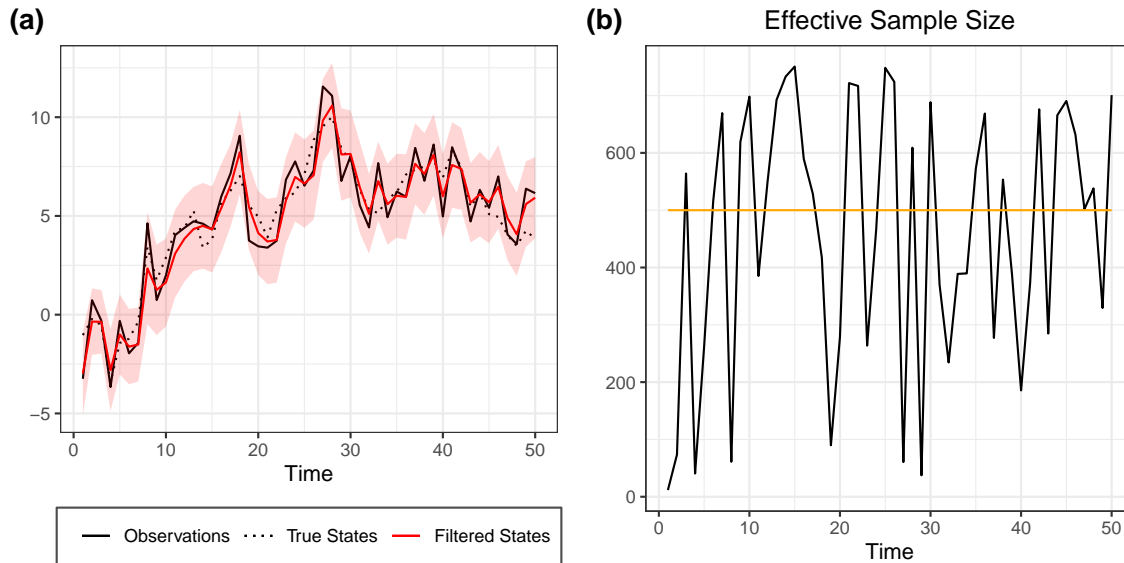


Figure 3.9: a) LW Filtered States with credible interval (in red). b) Effective sample size (in black) with threshold (in yellow).

Finally, we compare the performances of the Liu and West filter and the other filtering strategies discussed so far. As we expect, in the linear Gaussian case, Kalman filter outperforms the other strategies. On the other hand, the Liu and West, with hyperparameters setted as described above, provides the worst estimates in terms

of RMSE. This is not necessarily due to an overall weakness of the LWF with respect to the other filters, but simply to a not accurate choice of the hyperparameters. Moreover, while increasing the number of particles improves the accuracy, notice that the threshold for ESS-based resampling is not strictly related to better performances.

Table 3.4: RMSE

| N | Threshold | KF | BPF | APF | LWF |
|---|---|---|---|---|---|
| 100 | 0.50 | 0.879 | 0.916 | 0.881 | 0.883 |
| 1000 | 0.50 | 0.879 | 0.882 | 0.899 | 0.977 |
| 10000 | 0.50 | 0.879 | 0.885 | 0.874 | 0.945 |
| 1000 | 0.50 | 0.879 | 1.172 | 1.677 | 1.140 |
| 1000 | 0.25 | 0.879 | 1.085 | 0.974 | 3.419 |
| 1000 | 0.10 | 0.879 | 4.285 | 0.994 | 1.142 |

## 3.4 Convergence

## 3.5 Implementations for Stochastic Volatility Models

So far we have seen Sequential Monte Carlo methods applied to the linear Gaussian case, however, as already mentioned, for this class of state space models, Kalman Filter provides a closed form solution. Here, we want to provide an illustration of Particle Filters for a state space model for which no analytical solutions are available. More precisely, we deal with a stochastic volatility model. For the sake of simplicity we use a basic specification of stochastic volatility model

$$y_t|x_t \sim N(0, e^{\frac{x_t}{2}}) \tag{3.19}$$

$$x_t|x_{t-1} \sim N(\alpha + \beta x_{t-1}, \tau^2) \tag{3.20}$$

We start describing the main four particle filtering strategies discussed in this work and then we are going to compare their performances. The R code of these and other algorithms used in the Chapter application can be found in Appendix 1.

In the Bootstrap Particle filter we basically use the model transition kernel and do resampling any time the effective sample size is smaller than a predetermined threshold.

**Algorithm**  *BPF for Stochastic Volatility Model*

- *Let $\{(x_0, w_0)^{(i)}\}_{i=1}^N$ summarize $p(x_0|y_0)$ such that, for example, $E(g(x_0)|y_0) \approx \sum_{i=1}^N w_0^{(i)} g(x_0^{(i)})$. In particular, initialize $(x_0^{(1)}, ..., x_0^{(N)})$ form $N(m_0, C_0)$ and set $w_0^{(i)} = N^{-1} \ \forall \ i = 1, ..., N$.*

- *For t = 1, ..., n:*

  1. *Draw $x_t^{(i)} \sim N(\alpha + \beta x_{t-1}, \tau^2)$ $i = 1, ..., N$ such that $\{(x_t, w_{t-1})^{(i)}\}_{i=1}^N$ summarizes $p(x_t|y_{1:t-1})$*

  2. *Set $w_t^{(i)} = w_{t-1}^{(i)} f_N(y_t; 0, e^{\frac{x_t}{2}})$ $i = 1, ..., N$ such that $\{(x_t, w_t)^{(i)}\}_{i=1}^N$ summarizes $p(x_t|y_{1:t})$*

  3. *Normalize the weights: $w_t^{(i)} = \frac{\tilde{w}_t^{(i)}}{\sum_{j=1}^N (\tilde{w}_t^{(j)})}$*

  4. *Compute $ESS = \left( \sum_{i=1}^N (w_t^{(i)})^2 \right)^{-1}$*

  5. *if $ESS < N/2$ then*

     (a) *Draw a sample of size N, $(x_t^{(1)}, ..., x_t^{(N)})$, from the discrete distribution $P(x_t = x_t^{(i)}) = w_t^{(i)}$, $i = 1, ..., N$*

     (b) *Reset the weights: $w_t^{(i)} = N^{-1}$, $i = 1, ..., N$.*

  6. *Set $p(x_t|y_{1:t}) = \sum_{i=1}^N w_t^{(i)} \delta_{x_t^{(i)}}$*

If we instead want to sample from the optimal transition kernel, things get more complicated. It can be shown that the optimal transition kernel is

$$m_t^{opt}(x_t|x_{t-1}) \propto f_t(y_t|x_t) p(x_t|x_{t-1}) \propto exp\left[ -\frac{1}{2\sigma^2}(x_t - \alpha - \beta x_{t-1})^2 - \frac{e^{-x_t}}{2}y_t^2 - \frac{x_t}{2} \right]$$

and it is not straightforward to sample from it.

**Algorithm**  *GPF for Stochastic Volatility Model*

- *Let $\{(x_0, w_0)^{(i)}\}_{i=1}^N$ summarize $p(x_0|y_0)$ such that, for example, $E(g(x_0)|y_0) \approx \sum_{i=1}^N w_0^{(i)} g(x_0^{(i)})$. In particular, initialize $(x_0^{(1)}, ..., x_0^{(N)})$ from $N(m_0, C_0)$ and set $w_0^{(i)} = N^{-1} \ \forall \ i = 1, ..., N$.*

- *For t = 1, ..., n:*

  1. *Draw $x_t^{(i)} \sim N(\alpha + \beta x_{t-1} + \frac{\tau^2}{4}\left[y_t^2 e^{-(\alpha+\beta x_{t-1})} - 2\right], \tau^2)$ $i = 1, ..., N$ such that $\{(x_t, w_{t-1})^{(i)}\}_{i=1}^N$ summarizes $p(x_t|y_{1:t-1})$*

2. *Set $w_t^{(i)} = w_{t-1}^{(i)} \dfrac{f_N(y_t;0,e^{\frac{x_t}{2}})f_N(x_t;\alpha+\beta x_{t-1},\tau^2)}{f_N(x_t;\alpha+\beta x_{t-1}+\frac{\tau^2}{4}\left[y_t^2 e^{-(\alpha+\beta x_{t-1})}-2\right],\tau^2)}$  $i = 1,...,N$ such that $\{(x_t,w_t)^{(i)}\}_{i=1}^N$ summarizes*
   $p(x_t|y_{1:t})$

3. *Normalize the weights:* $w_t^{(i)} = \dfrac{\tilde{w}_t^{(i)}}{\sum_{j=1}^N (\tilde{w}_t^{(j)})}$

4. *Compute $ESS = \left(\sum_{i=1}^N (w_t^{(i)})^2\right)^{-1}$*

5. *if $ESS < N/2$ then*

   (a) *Draw a sample of size N, $(x_t^{(1)},...,x_t^{(N)})$, from the discrete distribution $P(x_t = x_t^{(i)}) = w_t^{(i)}$, $i = 1,...,N$*

   (b) *Reset the weights: $w_t^{(i)} = N^{-1}$, $i = 1,...,N$.*

6. *Set $p(x_t|y_{1:t}) = \sum_{i=1}^N w_t^{(i)}\delta_{x_t^{(i)}}$*

**Algorithm** *APF with optimal transition kernel for Stochastic Volatility Model*

- *Let $\{(x_0,w_0)^{(i)}\}_{i=1}^N$ summarizes $p(x_0|y_0)$ such that, for example, $E(g(x_0)|y_0) \approx \sum_{i=1}^N w_0^{(i)}g(x_0^{(i)})$. In particular, initialize $(x_0^{(1)},...,x_0^{(N)})$ from $N(m_0,C_0)$ and set $w_0^{(i)} = N^{-1} \,\forall\, i = 1,...,N$.*

- *For $t = 1,...,n$:*

   1. *Compute $ESS = \left(\sum_{i=1}^N (w_t^{(i)})^2\right)^{-1}$*

   2. *if $ESS < N/2$ then*

      (a) *Draw $I_k$ with $P(I_k = i) \propto w_{t-1}^{(i)} f_N(y_t|g(x_{t-1}^{(i)}),\sigma^2+\tau^2)$*

      (b) *Compute $\mu_{opt} = \mu(x_{t-1}^{(I_k)})$*

      (c) *Draw $x_t^{(k)} \sim N(\mu_{opt},\sigma_{opt}^2)$*

      (d) *Set $\tilde{w}_t^{(i)} = N^{-1}$ for $i = 1,...,N$*

   3. *otherwise*

      (a) *Compute $\mu_{opt} = \mu(x_{t-1})$*

      (b) *Draw $x_t^{(i)} \sim N(\mu_{opt},\sigma_{opt}^2)$ for $i = 1,...N$*

      (c) *Set $\tilde{w}_t^{(i)} = w_{t-1}^{(i)} f_N(y_t;x_t^{(i)},\sigma^2+\tau^2)$ for $i = 1,...,N$*

   4. *Normalize the weights:* $w_t^{(i)} = \dfrac{\tilde{w}_t^{(i)}}{\sum_{j=1}^N (\tilde{w}_t^{(j)})}$

**Algorithm** *LWF for Random Walk plus Noise Model*

- *Initialize $(x_0^{(1)}, ..., x_0^{(N)})$ from $N(m_0, C_0)$, $(\alpha^{(1)}, ..., \alpha^{(N)})$ from $N(e_\alpha, v_\alpha)$ and $(\beta^{(1)}, ..., \beta^{(N)})$ from $N(e_\beta, v_\beta)$ $(\tau^{2(1)}, ..., \tau^{2(N)})$ from $IG(v_0/2, v_0\lambda/2)$. Set $w_0^{(i)} = N^{-1}$ $\forall$ $i = 1, ..., N$ and chose the appropriate value for $\delta$. Therefore $\psi^{(i)} = (\alpha^{(i)}, \beta^{(i)}, \tau^{2(i)})$, and $\hat\pi_0 = p(x_0|y_0) = \sum_{i=1}^N w_0^{(i)} \delta_{(x_0^{(i)}, \psi^{(i)})}$*

- *For $t = 1, ..., n$:.*

    1. *Compute $\overline\psi = E_{\hat\pi_{t-1}}(\psi)$ and $\Sigma = V_{\hat\pi_{t-1}}(\psi)$. For $i = 1, ..., N$, set*

    $$m^{(i)} = a\psi^{(i)} + (1-a)\hat\psi$$
    $$\hat x_t^{(i)} = E(x_t|x_{t-1} = x_{t-1}^{(i)}, \psi = \psi^{(k)})$$

    2. *For $k = 1, ..., N$:*

        - *Draw $I_k$, with $P(I_k = i) \propto w_{t-1}^{(i)} f_N(y_t|0, e^{\frac{\hat x_t^{(i)}}{2}})$*

        - *Draw $\psi^{(k)}$ from $N(m^{(I_k)}, h^2\Sigma)$*

        - *Draw $x_t^{(k)}$ from $N(\alpha^{(k)} + \beta^{(k)} x_{t-1}^{(I_k)}, \tau^2)$*

        - *Set $\tilde w_t^{(k)} = \frac{f_N(y_t|0, e^{\frac{x_t^{(k)}}{2}})}{f_N(y_t|0, e^{\frac{\hat x_t^{(I_k)}}{2}})}$*

    3. *Compute $ESS = \left( \sum_{i=1}^N (w_t^{(i)})^2 \right)^{-1}$*

    4. *if $ESS < N/2$ then*

        (a) *Draw a sample of size N, $(x_t^{(1)}, ..., x_t^{(N)})$, from the discrete distribution $P(x_t = x_t^{(i)}) = w_t^{(i)}$, $i = 1, ..., N$*

        (b) *Reset the weights: $w_t^{(i)} = N^{-1}$, $i = 1, ..., N$.*

    5. *Set $\hat\pi_t = p(x_t|y_{1:t}) = \sum_{i=1}^N w_t^{(i)} \delta_{(x_t^{(i)}, \psi^{(i)})}$*

# Chapter 4

# Applications to Stochastic Volatility Models

## 4.1   Overview

In the following sections, we will try to replicate some of the analyses which were previously conducted on synthetic data, generated by a basic stochastic volatility model; this time, the same model specification and filters will be used on real data. However, as we will see, real data require different strategies to evaluate the effectiveness of several Sequential Monte Carlo techniques. Intuitively, such differences are due to the fact that now the latent process driving the Hidden Markov Model is not observed, nor do we know exactly its law of motion.

This part of the analysis is structured as follows: section *fill with the number of the section* provides a review of recent research in the stochastic volatility literature, including extensions of the basic specification and the use of particle filters; section *fill with the number of the section* describes the data which we employ and the transformations that were applied to them. In section *fill with the number of the section* we briefly compare the series of filtered states that are obtained from different particle filters; moreover, several PFs are compared in terms of computational cost in approximating the exact filtering distribution implied by our SV model. Section *fill with the number of the section* features a forecast comparison between two SV specifications and a model that assumes constant mean and variance for the financial returns, namely a forecasting exercise that would not be possible were it not for particle filtering techniques. In section *fill with the number of the section* we

conclude by employing a non-parametric measure of realised volatility as a proxy for the latent volatility process, allowing a RMSE and MAE comparison between filters which is similar to that of section *fill with the number of the section* for synthetic data.

## 4.2    A review of Stochastic Volatility models

In section *fill with the number of the section* a simple specification of a Stochastic Volatility model was presented and used as the data generating process of a simulated dataset. Denoting by $y_t$ the log returns at time $t$ and by $x_t$ the latent volatility stochastic process, such state-space model was presented as follows,

$$y_t | x_t \sim N(0, e^{x_t})$$

$$x_t | x_{t-1}, \alpha, \beta, \tau^2 \sim N(\alpha + \beta x_{t-1}, \tau^2)$$

This specification - which we will employ in this section on a real dataset - can be deemed as the standard version of the SV model. Throughout the recent decades, several extensions have been proposed, mostly (but not exclusively) in the field of financial econometrics. On the one hand, for simplicity we will stick to the standard version, one that will suffice for the scope of this work on Sequential Monte Carlo methods. On the other hand, it is worth mentioning some of these extensions: indeed, one can rather safely assume that, through their higher degree of sophistication, such extensions might well improve on the performance of our standard SV model in the analyses that will follow.

Stochastic Volatility Models, whose early formulation is commonly attributed to Taylor (1982, 1986), allow to account for time-varying and autoregressive volatility in financial returns, posing themselves as a valid alternative to ARCH (Engle 1982) or GARCH (Bollerslev 1986) models in dealing with non-constant volatility. Kim, Shephard and Chib (1998) define the canonical model for regularly spaced data as

$$y_t = \psi e^{\frac{x_t}{2}} \epsilon_t$$

$$x_{t+1} = \mu + \beta(x_t - \mu) + \tau \eta_t$$

$$x_1 | \sigma, \beta \sim N\left(\mu, \frac{\sigma^2}{1 - \beta^2}\right)$$

$$\epsilon_t \sim N(0, 1)$$

$$\eta_t \sim N(0, 1)$$

where the log volatility $x_t$ is assumed to follow a stationary process ($|\beta| < 1$), $\psi$ is a constant scaling factor, $\beta$ is

the persistence in the volatility and $\tau$ is the volatility of the log-volatility.[1] Most importantly, $\epsilon_t$ and $\eta_t$, the Gaussian white noise processes that drive the canonical model, are assumed to be uncorrelated. This latter assumption justifies another definition of this specification, namely "discrete SV model without leverage".[2] In order to accommodate for leverage effects, namely capture the increase in volatility that follows a drop in the returns, the model can extended as in Omori et al. (2007),

$$y_t = e^{\frac{x_t}{2}} \epsilon_t$$

$$x_{t+1} = \mu + \beta(x_t - \mu) + \eta_t$$

$$\begin{pmatrix} \epsilon_t \\ \eta_t \end{pmatrix} \Big| \rho, \tau \stackrel{i.i.d.}{\sim} N_2(\mathbf{0}, \Sigma), \ \Sigma = \begin{pmatrix} 1 & \rho\tau \\ \rho\tau & \tau^2 \end{pmatrix}$$

where $\rho < 0$ captures the negative correlation. Such specification, which can be referred to as "discrete SV model with leverage", captures the asymmetric response of volatility to returns of different signs, so that similar specifications are sometimes also deemed as "asymmetric SV models" (e.g. Harvey and Shephard 1996, Mao et al. 2020).

Note that so far the assumptions on $\epsilon_t$ and $\eta_t$ implied that the returns are conditionally normally distributed. The discrete time SV models can also be extended to allow for heavy-tailed or asymmetric conditional returns distributions: symmetric or skewed Student-$t$, Generalised Hyperbolic (GH) distribution, Generalised Error Distribution (GED) and scale mixtures of normals feature as popular choices (Kim and Stoffer 2008, Nakajima and Omori 2012, Mao et al. 2020). In fact, SV with heavy tailed return distributions were shown to better meet empirical regularities like the leptokurtic distribution of the returns and slowly decaying autocorrelation functions of the squared returns (Liesenfeld and Jung 2000).

Assuming that $\epsilon_t$ follows a Student-$t$ distribution, and exploiting the fact that $\epsilon_t$ can then be written as $\lambda_t^{-1/2} \zeta_t$, where $\zeta_t \sim N(0, 1)$ and $\nu\lambda_t \sim \chi_\nu^2$ (Harvey et al. 1994, Chib et al. 2002), we have the following SV model with

---

[1]For identifiability reasons, either $\psi = 1$ or $\mu = 0$. Kim, Shephard and Chib (1998) prefer $\psi = 1$.

[2]Note that in this review we do not focus on continuous time SV models. In fact, such models have attracted a considerable amount of research in financial econometrics and mathematical finance, especially after Hull and White (1987) considered stochastic volatility for option pricing. Arguably, the most influential model was then proposed for option pricing by Heston (1993), a SV model with leverage effects and square root diffusion driving volatility. Diffusion-based SV models enjoyed increasing popularity, see for example Barndorff-Nielsen and Shephard (2001), or Christoffersen et al. (2010), who investigate alternatives to the entrenched affine square root SV model. Eraker (2004) proposed a SV model with correlated jumps in prices and volatility, extending Heston's model, while Comte and Renault (1998) extended Hull and White's model as to feature long memory properties. More recently, Gatheral et al. (2018) further built on Comte and Renault's fractional SV model to propose the popular "rough volatility models" (see also Friz et al., 2021).

both fat tails and leverage effect (Jacquier et al., 2004),

$$y_t = e^{\frac{x_t}{2}} \lambda_t^{-1/2} \zeta_t$$

$$x_{t+1} = \alpha + \beta x_t + \eta_t$$

$$\begin{pmatrix} \zeta_t \\ \eta_t \end{pmatrix} \bigg| \rho, \tau \overset{i.i.d.}{\sim} N_2(\mathbf{0}, \Sigma), \ \Sigma = \begin{pmatrix} 1 & \rho\tau \\ \rho\tau & \tau^2 \end{pmatrix}$$

$$v\lambda_t \sim \chi_v^2$$

To capture other elements of the behaviour of financial data, several other extensions have been proposed. For example, SV models have been extended to include conditional heteroskedasticity in the mean returns (Koopman and Hol Uspensky 2002) to capture potential volatility feedback effects, or to feature autoregressive moving average innovations (Chan 2013, Zhang et al. 2020), allowing better goodness of fit and out-of-sample forecasts.[3] [4] The model proposed by Koopman and Hol Uspensky is specified as

$$y_t = v_t + \psi e^{\frac{x_t}{2}} \epsilon_t$$

$$v_t = a + by_{t-1} + d\psi^2 e^{x_t}$$

$$x_t = \beta x_{t-1} + \tau \eta_t$$

$$\begin{pmatrix} \epsilon_t \\ \eta_t \end{pmatrix} \overset{i.i.d.}{\sim} N_2\left(\mathbf{0}, \begin{pmatrix} 1 & 0 \\ 0 & 1 \end{pmatrix}\right)$$

while the state space representation of the ARMA(p,q)-SV framework, as in Zhang et al. (2020), reads

$$y_t = v_t + \gamma_t$$

$$\gamma_t = \phi_1 \gamma_{t-1} + ... + \phi_p \gamma_{t-p} + u_t + \varphi_1 u_{t-1} + ... + \varphi_q u_{t-q}$$

$$u_t | x_t \sim N(0, e^{x_t})$$

$$x_t = x_{t-1} + \eta_t$$

$$\eta_t | \tau \sim N(0, \tau^2)$$

---

[3]Dimitrakopoulos and Kolossiatis (2020) note that "the moving average component, the leverage effect and the conditional heteroscedasticity in mean have been considered separately in the stochastic volatility literature" and provide two specifications, one featuring an MA component and leverage effects, the other an MA component and conditional heteroskedasticity in mean.

[4]Other extensions, though ones for which we do not report the specifications, feature modelling the latent volatility process $x_t$ as an ARFIMA process (Long Memory Stochastic Volatility model, Breidt et al. 1998) or as governed by a first-order Markov process (Markov Switching Stochastic Volatility model, So et al. 1998). Recently, Luo et al. (2018) incorporated neural networks in the stochastic volatility model (Neural Stochastic Volatility Model), while Xu and Chen (2021) employ deep learning models (Deep Stochastic Volatility Model).

where the error terms $u_t$ and $\eta_t$ are independent across all leads and lags, while $\nu_t$ follows an unspecified time-varying process.

Interestingly enough, the path along which the SV models evolved coincides with that suggested by optimal portfolio findings. Johannes, Korteweg and Polson (2014) found that, in order to generate statistically significant portfolio improvements in a Bayesian learning problem, the model employed by the investor should incorporate both time-varying expected returns and stochastic volatility: indeed, either of these features alone did not lead to statistically significant gains with respect to employing models with time-constant expected returns and volatility.[5]

Finally, before moving to the application of Sequential Monte Carlo techniques to a SV model, we conclude by going through some references for the Bayesian analysis proposed for such models. Starting from the seminal work of Jacquier et al. (1994), the use of MCMC methods has become increasingly popular for parameter estimation and smoothing exercises in SV models (e.g. Kastner 2019, presenting the R package *stochvol* for Bayesian parameter estimation, and Chopin and Papaspiliopoulos 2020, who use MCMC to sample from the smoothing distribution of a SV model). As regards filtering exercises, the adoption of particle filters was rather rapid:[6] indeed, latent volatilities in Kim et al. (1998) were already filtered by employing the particle filter suggested in Pitt and Shephard (1999), paving the way for subsequent applications (*inter alia*) in Chib et al. (2006), Omori et al. (2007), Kim and Stoffer (2008) and Nakajima and Omori (2012).

## 4.3 Data Description

As previously mentioned, we will analyze the behaviour of the described filtering tools associated to a simple stochastic volatility model. In particular, we are evaluating the performance of such model on real data. For the observable process, namely financial returns in the SV model, we consider the continuously compounded daily returns (also called logarithmic returns) of three indices, S&P500, DOW JONES and STOXX50, in a time interval from June 1st, 2017 to May 30th, 2021. From these, we estimate the daily volatility, as computed

---

[5]One could then argue that caution is needed when employing basic specifications of stochastic volatility models. For instance, Poon and Granger (2005) found that historical volatility and ARCH models both achieved better volatility forecasting performance than SV models. Similarly, Allen and McAleer (2020, see also Allen, 2020) found that, using realised volatility as benchmark, neither the canonical SV model or a GARCH(1,1) specification could forecast better than a simple form of historical volatility model.

[6]Actually, SV models are now often used as straightforward applications of particle filters on non-linear state space models, see for example Andrieu et al. (2010), Douc et al. (2014) or Chopin and Papaspiliopoulos (2020).

by the model.

The indices have been selected as representatives of the global economic trends in the US and EU markets. Specifically, the S&P500 is a market-capitalization-weighted stock-price index tracing the performance of the 500 largest companies listed on US stock exchanges (NYSE and Nasdaq Exchange). The DOW JONES, instead, is a price-weighted stock-market index and accounts for the 30 major companies listed on US stock exchanges, characterized for being "blue-chip". Also the EURO STOXX 50 follows bluce-chip stocks representing leading firms in regions of the Eurozone.

The three plots below represent the time series of the log returns calculated for the three indices during our period of interest. In particular, each series is a sequence of daily observations representing the logarithm of the ratio between the closing price of the index for a given day and the closing price of the day before.
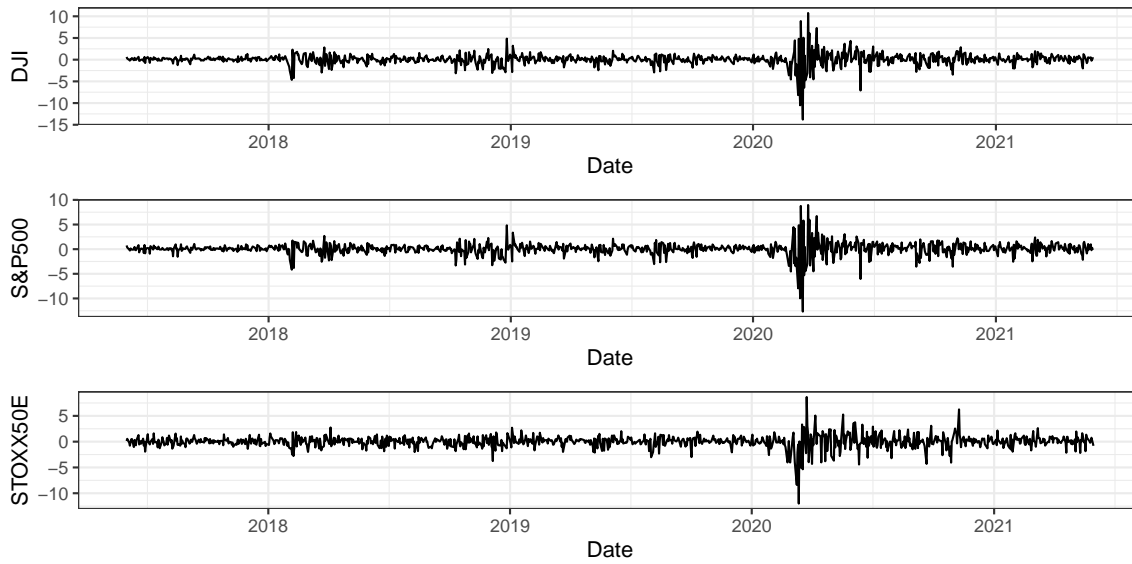


Figure 4.1: Close to close percentage log returns, 3 indices

At a first visual inspection, we can see a common behaviour in the volatility of all three indices. Especially, it is worth pointing out the similarity between the pattern of DJI and that of S&P500 (especially in terms of peaks), which both differ from the STOXX50E, presumably because the first two describe the US stock market, while the last index describes the European one. For example, a difference that can be seen by having a glance at the plots is that the US indices log returns displays differences in fluctuation magnitude across

different periods that are more marked than for the EU index, for which log returns display, in general, wider fluctuations. Anyways, what stands out the most in all three plots is the very wide fluctuations present from February - March 2020 to around September 2020, which, very intuitively, are connected with the Covid-19 Pandemic Crisis.

Table 4.1: Summary statistics, close to close percentage log returns

|                    | S&P500  | Dow Jones | STOXX50E |
| ------------------ | ------- | --------- | -------- |
| Mean               | 0.05581 | 0.05002   | 0.01229  |
| Standard Deviation | 1.32564 | 1.38510   | 1.22951  |

As regards the series that we will employ in section *fill with the number of the section*, namely the series of realised volatilities which we will employ as a proxy for the true latent volatilities, the data were retrieved from the Oxford-Man Institute's Realized Library, which provides several different daily non-parametric measures of past volatility.[7] We consider a proper rescaling of the *rv5* series, *i.e.* model-free daily volatility estimates based on 5 min intraday return intervals. Also in this case, the chosen interval spanned from June 1st, 2017 to May 30th, 2021. The plots below represent the realized volatility in the period of interest for all the three indices.[8] As usual, they show a rather similar pattern across all three indices, identifying peaks corresponding to periods of higher uncertainty (in particular referring to the 2020 Covid-19 Crisis outbreak and its impact over time). Once more, there is great similarity between the series for the DJI and the one for the S&P500, while the series of the STOXX50E appears slightly different, in terms of peaks.

---

[7] Such class of measures will be better presented in section *fill with the number of the section*, when reviewing the use of realised volatility estimators as proxies for latent volatilities.

[8] In the graph, the series *rv5* is rescaled as specified in the upcoming section: we took the square root of each value, which is a daily variance measure, and multiplied it by 100.
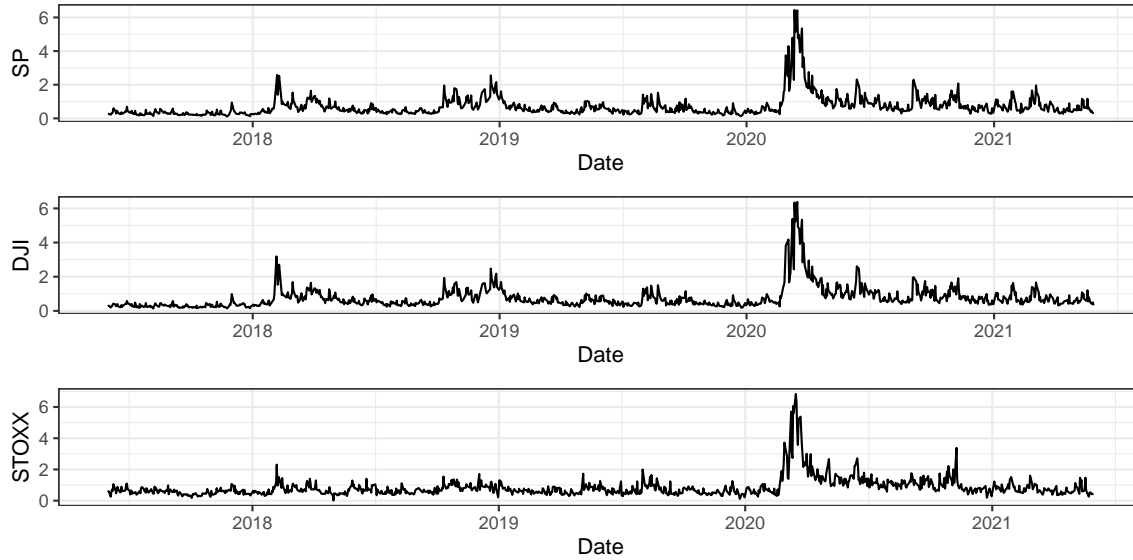
Figure 4.2: Rescaled realised daily volatility, 3 indices

## 4.3.1 Rescaling the data

When specifying the parameters of a stochastic volatility model, one should clarify whether the series of observed financial returns is one of log returns or of percentage log returns. Indeed, let $y_t$ denote the returns at time $t$, so that a basic SV specification would prescribe $y_t|x_t \sim N(0, e^{x_t})$: clearly, for each period $t$, $e^{x_t}$ needs to be higher to replicate the observed *percentage* log return rather than the observed log return. This implies that the latent volatility $x$ should fluctuate around higher values when using percentage log returns as $y_t$. This feature, when adopting the aforementioned canonical SV model as defined in Kim et al. (1998), would be represented by a higher $\mu$. For example, as noted in Kastner (2019), daily log returns often have a variance of 0.0001 or less, which implies that $\mu$ should lie somewhere around $\ln(0.0001) \approx -9$; instead, when considering daily percentage log returns, one then has a variance of 1, so that $\mu = \ln(1) = 0$. In other terms, one might end up with a basic specification of the SV model when (roughly) calibrating the parameters of the canonical model on a wider set of financial returns.

Note that rescaling the log returns has analogous implications for the section in which we employ measures of realised volatility as a proxy for the latent volatility process. Let us denote by $rv5_t$ the daily realised variance at time $t$, which we obtain from the $rv5$ series provided in the Oxford-Man database. Now, note that in a SV framework one should not directly compare $rv5_t$ to $x_t$, as $rv5_t$ can be rather seen as an estimate of the variance

of the log returns at time $t$, *i.e.* of $e^{x_t}$ in the SV model.[9] Moreover, by construction of $rv5_t$, the comparison should feature a SV model where the log returns did *not* undergo the percentage transformation.[10] Thus, in order to achieve a common scale with the percentage log returns, we need to multiply $rv5$ by $100^2$. To ease the interpretation and representation of the comparison between differently approximated filtering distributions, we finally take the square root of the rescaled $rv5$, so that we compare it to $e^{x_t/2}$.

## 4.4 Comparing the filters

In this section the different particle filter techniques we discussed in earlier sections will be employed to approximate the filtering distribution that springs from a simple SV model applied to a real dataset. First, we provide a qualitative comparison between the filters, basing on visual analysis of the (approximated) filtering distributions. Subsequently, we move to a more quantitative approach, in order to assess the quality of the approximations as the number of particles increases. In a way, while in the first part most filters can be rather confidently assumed to be close to convergence, the second subsection will hint at possibly different computational costs across the competing filters.

Before moving to such analyses, it is worth mentioning that not all the filters we employ approximate the same filtering distribution $p(x_t|y_{1:t}, \psi)$, where $\psi$ is a vector containing the parameters of the model. Indeed, the Liu and West filter actually approximates the distribution of a slightly different SV model, one that assumes an additional hierarchical level,

$$y_t|x_t \sim N(0, e^{x_t})$$
$$x_t|x_{t-1}, \alpha, \beta, \tau^2 \sim N(\alpha + \beta x_{t-1}, \tau^2)$$
$$x_0 \sim N(0, 100)$$
$$\alpha \sim N(\gamma, \zeta)$$
$$\beta \sim N(\pi, \phi)$$
$$\tau^2 \sim IG(\nu/2, \lambda\nu/2)$$

where $\gamma, \zeta, \pi, \phi, \nu$ and $\lambda$ are assumed to be known.[11]

---

[9]See for example Guidolin and Pedio (2021), who employ $rv10$, another measure of realised volatility provided in the Oxford-Man Library, as a proxy for the latent conditional variance of the daily log returns on the FTSE100 index.

[10]Indeed, this estimator is based on the sum of 5-minute intra-day squared returns: such returns are computed as the difference between the opening and closure price in an interval.

[11]In these empirical applications we keep the values of the parameter we employed in the synthetic data part, see section *fill with the number of the section*

### 4.4.1   Visual Analysis after Filtering

We now offer a preliminary comparison of the various filtering methods, based on a visual analysis of graphs representing, for each index, the time-varying volatility of the observations, obtained through the application of the different filtering techniques explored in the theoretical analysis. Plots that are compared represent the sequence of percentage log returns for a given index (the observations, in gray) and the sequence of filtered volatilities calculated using filtered states (in red) obtained through a specific filtering technique indicated in the caption of the plot.[12]

First, a general point is that the sequence of percentage log returns are different across the three indices. The reasons why this holds can be associated with the index-construction method and the characteristics of the economy and industrial setting it represents (SEE SECTION X). In particular, as previously noticed, there are extensive similarities between the DOW JONES Index and the S&P500, which can be visualized when looking at the percentage of log returns in the corresponding plots, since both are describing the US Economy. However, the STOXX50E differs quite extensively, especially in the different sensitivity to the Covid-19 Crisis and its consequences, representing the European Economy. Aside from this note, the considerations expressed below on the sequences "filtered volatilities"[13] for the various techniques hold almost uniformly for all the three indices. Therefore, in the next paragraph we will be referring to the set of plots pertaining to one specific index (which could be any of the three).

Generally speaking, note that, the sequence of "filtered volatilities" obtained from any of the filtering techniques follows roughly similar paths across all the plots. Unsurprisingly, the filtered volatility appears wider in periods corresponding to wider fluctuations of the percentage log returns and lower in periods corresponding to smaller such fluctuations. For example, all sequences of filtered volatilities show peaks corresponding to the higher fluctuations due to the 2020 Covid-19 Crisis outbreak and the consequent increases in uncertainty for the later periods.

When focusing the attention on specific filters, first we can discuss the effect of resampling. Indeed, in the plot referring to the Sequential Importance Sampling procedure, the sequence of filtered volatilities is not able to

---

[12]Such filtered volatilities are obtained as follows. For each $t$, let us denote by $\mu_t$ the mean of the generated particles; the filtered volatility is then defined as $e^{\mu_t}$. Note that the number of particles was set at 10000 for each filter: the conclusion of the next section will come back to such a choice.

[13]Per ora nei grafici c'è scritto "Filtered States", verrà corretto.

reproduce the peaks as in with other filters, but also is characterized by collapsing confidence intervals. This is because :::::::

Then, if we instead look at the filtered volatilities obtained with resampling, we can appreciate how the filtered sequences for the Basic,[14] Bootstrap, Auxiliary and Optimal Kernel Guided particle filters give rather analogous results, with no differences appearing at a first visual inspection.[15]

However, the sequence of filtered volatilities obtained by applying the Liu and West filter is clearly different from the others. Indeed, it shows a "more detailed" sequence of states (in the sense of the sequence of filtered volatilities being less smooth) and also a higher peak for the wide fluctuation corresponding to the 2020 Covid Crisis outbreak. Therefore, we may expect that, compared to other filtering techniques, it can provide a better representation of the data. This is because . . . *Potremmo parlare di maggiore sensibilità alle oscillazioni dei prezzi, o simili*

### 4.4.2 Quality of approximation

Since we do not have access to the exact filtering distribution of the SV model, when assessing how rapidly different particle filters converge to it, we actually need to approximate even such target distribution as to have a benchmark.

Fortunately, convergence results about particle filters ensure that when the number of particles diverges, the approximation converges to the target distribution.[16] Thus, we run one of the particle filters with a very large number of particles, and assume that such approximation is close enough to the target to be used itself as the distribution the filters should tend to.

With such a benchmark, we can then compare how different filters approach it as the number of particles increases. We employ the Root Mean Squared Error and the Mean Absolute Error to measure discrepancies from the benchmark. Note that the Liu and West filter can not be included in such an analysis: trivially, the comparison assumes that the competing algorithms are approximating the same target distribution.[17]

We start by running the Bootstrap particle filter with N=50000, setting it as the benchmark. In table XX we

---

[14]By this name, we refer to a particle filter that features no adaptive resampling; rather, resampling is conducted at each step of the algorithm.

[15]Except for the Auxiliary Particle filtered sequence of volatilities, showing a slightly higher peak corresponding to the greatest volatility fluctuation in 2020, if compared to other filters in this subset. This is still valid for all three indices.

[16]Molto probabilmente la frase formulata così non è formalmente corretta...bisognerebbe fare riferimento alla sezione sulla convergenza. Inoltre, va chiarito il punto della "doppia convergenza".

[17]For an analogous reason, we do not need to conduct this analysis on all the indices, but we can rather focus on one, the SP500. Indeed, what matters in this section is not how well the model fits the data, but rather how different algorithms approach the same distribution yielded by the same model on a given set of data.

report the RMSE and MAE measures one obtains by comparing the mean of the particles generated at each step by the Bootstrap PF with N=50000 and the mean[18] of the particles generated by other particles filters with N equal to 10, 100, 1000, 5000 or 10000.[19]

Table 4.2: RMSE and MAE, Bootstrap PF 50000 particles

|        | N     | BPF     | GPFOPT  | APF     | BAPF    | SIS     |
|--------|-------|---------|---------|---------|---------|---------|
| RMSE   | 10    | 0.42331 | 0.36853 | 0.54784 | 0.55959 | 0.91686 |
| RMSE   | 100   | 0.15689 | 0.15094 | 0.24044 | 0.23488 | 1.10551 |
| RMSE   | 1000  | 0.06901 | 0.07669 | 0.08878 | 0.10295 | 0.62505 |
| RMSE   | 5000  | 0.03817 | 0.03568 | 0.05742 | 0.06110 | 0.62004 |
| RMSE   | 10000 | 0.03045 | 0.02709 | 0.04296 | 0.05151 | 0.51189 |
| MAE    | 10    | 0.28078 | 0.27961 | 0.43103 | 0.43779 | 0.72753 |
| MAE    | 100   | 0.09658 | 0.09624 | 0.17570 | 0.18394 | 0.91799 |
| MAE    | 1000  | 0.03312 | 0.03697 | 0.05539 | 0.06726 | 0.49718 |
| MAE    | 5000  | 0.01889 | 0.01665 | 0.03186 | 0.03448 | 0.44753 |
| MAE    | 10000 | 0.01456 | 0.01423 | 0.02449 | 0.02726 | 0.40636 |

As we can see, almost every filter shows dramatic improvement already when passing from 10 particles to 100 particles, while the performance of the SIS algorithm actually gets worse. With N=10 or N=100, the Bootstrap PF and the Guided PF (with optimal proposal kernel) emerge quite clearly as the best performing filters; however, no conclusion should be drawn at this stage, as the large errors seem to suggest quite a wide margin from improvement even for the best performing filters.

As it turns out, such suggestion is confirmed by running the algorithms with N=1000. Passing from 100 to 1000 particles more than halves the RMSEs across the 5 competing filters, with even more pronounced gains in the MAEs; at N=1000, the Bootstrap and the Guided particle filters still hold their lead over the rest of the

---

[18]As a possible limitation of our exercise, here we do not consider in detail the variance of such generated particles. Nevertheless, one can get at least an idea of the differences in the generated variances by comparing the confidence intervals that will be shown in the graphs below. Unsurprisingly, it will be apparent that including a resampling step is essential to avoid a collapsing effective sample size.

[19]We consider 5 algorithms: a Bootstrap PF, a Guided PF (with the optimal proposal kernel), an Auxiliary PF, a "Basic PF" and a Sequential Importance Sampling alogrithm. By "Basic PF" we refer to a Bootstrap PF that features resampling at each step, whereas resampling never happens in the SIS algorithm: one can then consider these 2 algorithms as extreme cases of an adaptive resampling algorithm, namely one that features resampling when $ESS$ is non negative (*i.e.* always) or when $ESS < 0$ (*i.e.* never). In this sense, we use the shorthand "particle filters" when referring to all the 5 algorithms.

field, keeping a shrinking hedge over the Auxiliary PF, which shows most impressive gains when passing from 100 to 1000 particles. Further sizable gains for every filter, except for the SIS algorithm, are observed when increasing the number of particles to 5000, a level at which both the RMSE and the MAE agree on a slight hedge of the Guided and the Bootstrap filters over the Auxiliary and the Basic PFs.

Nevertheless, we would argue that already for N=5000, but even more clearly for N=10000, the difference between the Bootstrap, the Guided and the Auxiliary particle filters is so small that none of these filters can be straightforwardly chosen over the others, a figure which visual inspection of the graphs below can confirm. Interestingly enough, no gains seem to arise from resampling at each step with respect to adaptive resampling (note that the Basic PF is preferred to the APF only once, by the RMSE), whereas the need of some degree of resampling is apparent, as shown by the awful performance of the SIS algorithm with any number of particles. Moreover, the RMSE and the MAE show infrequent disagreement, delivering a rather clear picture of the comparison.

Now, one might argue that the relative performance of the filters is influenced by the choice of the Bootstrap filter as the benchmark algorithm when run with N=50000: intuitively, if the convergence phase were not reached, the Bootstrap filter (which did in fact come out as one of the best performing algorithms) would clearly find it easier to replicate the benchmark we set.[20]

As a robustness check, we thus conduct the same analysis employing the Auxiliary Particle Filter as the benchmark, keeping the number of particles set to 50000 as for the benchmark BT filter.

Table 4.3: RMSE and MAE, Auxiliary PF 50000 particles

|       | N     | BPF     | GPFOPT  | APF     | BAPF    | SIS     |
|-------|-------|---------|---------|---------|---------|---------|
| RMSE  | 10    | 0.40549 | 0.34950 | 0.53237 | 0.54597 | 0.91038 |
| RMSE  | 100   | 0.13510 | 0.14209 | 0.22243 | 0.22398 | 1.10156 |
| RMSE  | 1000  | 0.04145 | 0.06874 | 0.07796 | 0.07692 | 0.61504 |
| RMSE  | 5000  | 0.02847 | 0.04922 | 0.03931 | 0.05230 | 0.61176 |
| RMSE  | 10000 | 0.03048 | 0.03337 | 0.02648 | 0.02411 | 0.50547 |
| MAE   | 10    | 0.27266 | 0.26941 | 0.42151 | 0.42909 | 0.72112 |
| MAE   | 100   | 0.08540 | 0.09034 | 0.16691 | 0.17484 | 0.91468 |
| MAE   | 1000  | 0.02329 | 0.03532 | 0.05105 | 0.05753 | 0.48959 |

---

[20]Note that all the filters, including the BT filter run with 50000 particles, shared the same seed in the *R* software, ruling randomness out of these considerations.

| | | | | | | |
|---|---|---|---|---|---|---|
| MAE | 5000 | 0.01756 | 0.02410 | 0.02662 | 0.03275 | 0.44195 |
| MAE | 10000 | 0.01417 | 0.01718 | 0.01974 | 0.01742 | 0.40221 |

Using the APF as the benchmark does not deliver a different picture than the one we previously had. Leaving the SIS algorithm aside (whose analogous performance comes as no surprise), it is interesting to note how once again the Auxiliary particle filter actually fares worse than the Bootstrap and the Guided PFs at 10, 100 and 1000 particles.

Its performance ameliorates dramatically at N=1000, while at N=5000 the halving of its RMSE and MAE even allows the APF to overtake the Guided PF, though falling short of the Bootstrap PF. At N=10000 both the Basic PF and the APF achieve lower RMSEs than the Bootstrap and the Guided PF, even though the MAE criterion still selects the Bootstrap as the closest to the target distribution.

Interestingly, this time the performance of the Bootstrap filter worsens when N is increased from 5000 to 10000 (both according to RMSEs and MAEs, whose disagreements, once again, are overall infrequent). Such evidence suggests that, even at very large (yet finite) values of N, some difference between the approximated filtering distributions still persists across our particle filters.

Table 4.4: Discrepancy between Bootstrap and Auxiliary PFs

| | RMSE | MAE |
|---|---|---|
| N=50000 | 0.04408 | 0.01668 |
| N=100000 | 0.03576 | 0.01476 |

In fact, by comparing the two benchmark approximations with N=50000, we can see that, for example, the Bootstrap PF run with N=10000 is closer to the benchmark APF than the benchmark BT is, or that the RMSE ranks the APF with N=10000 as closer to the the benchmark BT than the APF with N=50000, mildly pointing at a theoretically-unsound difference between the limiting distributions of the filters. Nevertheless, now the RMSE and MAE do not deliver unanimous verdicts, nor the differences seem large enough to back extreme claims. And, conveniently, running the Auxiliary and the Bootstrap filters with 100000 particles testifies a shrinking difference between the approximations - at increasingly large computational costs, though.

Overall, we should not overplay tiny differences.[21] Rather, we prefer to stress the points that emerged from both benchmark analyses and we can therefore support quite confidently.

First, if on the one hand it is clear that some degree of resampling is essential, on the other we found no gains from resampling at each period.

Second, when the number of particles is set at 5000 or more, neither benchmark could single out an algorithm that clearly outperformed the others, when restricting the analysis to procedures that feature adaptive resampling rules.

Third, when the number of particles was set to 10, 100 or 1000, the Bootstrap particle filter and the Guided particle filter with optimal proposal kernel significantly emerged as the best performing algorithms for our SV model, suggesting that their computational cost is lower than that of the Auxiliary particle filter, which needed more particles to "get rolling".

Finally, some discrepancy between different approximations persisted even when the number of particles was set to 50000 or 100000. However, the narrow extent of the RMSEs and MAEs with respect to both benchmarks supports the idea that at N=10000 the best-performing algorithms have already entered the phase of convergence. Even in light of these markedly more computationally expensive benchmarks, we then choose N=10000 as the number of particles which we routinely employ in this empirical application.

## 4.5 Comparing Constant and Stochastic Volatility Models of Equity Returns

In this section, we apply the particle filter in a model-comparison exercise, ultimately underlining the importance of taking stochastic volatility into account in modeling equity returns. We follow XX, comparing density forecasts through relative predictive and cumulative likelihoods.

We analyze a dataset of log close-to-close returns of the S&P500, from 2017 to 2021. Consider a stochastic volatility model

$$\mathcal{M}_{SV}: \begin{array}{l} r_t = \alpha_r + \sigma_{r,t} \cdot v_t \\ \log \sigma_{r,t}^2 = \alpha_\sigma + \beta_\sigma \cdot \log \sigma_{r,t-1}^2 + \sigma_\sigma \cdot w_t \end{array} \qquad (v_t, w_t) \sim \mathcal{N}_2(\mathbf{0}, I_2)$$

---

[21]Indeed, the mere extent of such difference also depends on the real dataset which is used for the comparison, implying different target distributions. For example, running the same experiment using the STOXX50E dataset, we have even smaller differences between the filters at N=50000, with RMS difference between the Bootstrap and the Auxiliary equal to 0.01236279 and mean absolute difference equal to 0.008028818.

and a constant volatility iid model

$$\mathcal{M}_{CV} : (r_t) \overset{iid}{\sim} \mathcal{N}(\alpha, \sigma^2).$$

We calibrate the model parameters using the whole sample, and proceed by setting the return mean of both models to equal the sample mean, $\sigma^2$ equal to the return variance, and the parameters of the volatility equation in $\mathcal{M}_{SV}$ by running an $AR(1)$ regression of the log squared residuals.

In order to compare the predictive performance of the two, we compare the cumulative log likelihood of the observed returns up to time $t$ given the considered model. In formulas, the cumulative likelihood can be computed as

$$p(y_{1:t}|\mathcal{M}_i) = \prod_{s=0}^{t-1} p(y_{s+1}|y_{1:s}, \mathcal{M}_i), i \in \{SV, CV\},$$

adopting the convention $y_{1:0} = \varnothing$. This is trivial to obtain in the iid case; considering the stohastic volatility model, the predictive likelihoods can be derived as

$$p(y_{t+1}|y_{1:t}, \mathcal{M}_{SV}) = \int p(y_{t+1}|\sigma_{r,t+1}, y_{1:t}, \mathcal{M}_{SV}) p(\sigma_{r,t+1}|y_{1:t}, \mathcal{M}_{SV}) d(\sigma_{r,t+1})$$

$$= \int p(y_{t+1}|\sigma_{r,t+1}\mathcal{M}_{SV}) p(\sigma_{r,t+1}|y_{1:t}, \mathcal{M}_{SV}) d(\sigma_{r,t+1})$$

Whereas the emission distribution $p(y_{t+1}|\sigma_{r,t+1}\mathcal{M}_{SV})$ is known, we approximate the predictive state distribution $p(\sigma_{r,t+1}|y_{1:t}, \mathcal{M}_{SV})$ with weighted particles obtained with particle filtering.

Figure XX reports the time series of the cumulative log-likelihood given the constant volatility model $\mathcal{M}_{CV}$ relative to the one given $\mathcal{M}_{SV}$, obtained as $\log p(y_{1:t}|\mathcal{M}_{CV}) - \log p(y_{1:t}|\mathcal{M}_{SV})$. Notice that the first difference of this series is the relative log-likelihood of the incoming observation, $p(y_t|y_{1:t-1}, \mathcal{M}_{CV}) - p(y_t|y_{1:t-1}, \mathcal{M}_{SV})$.
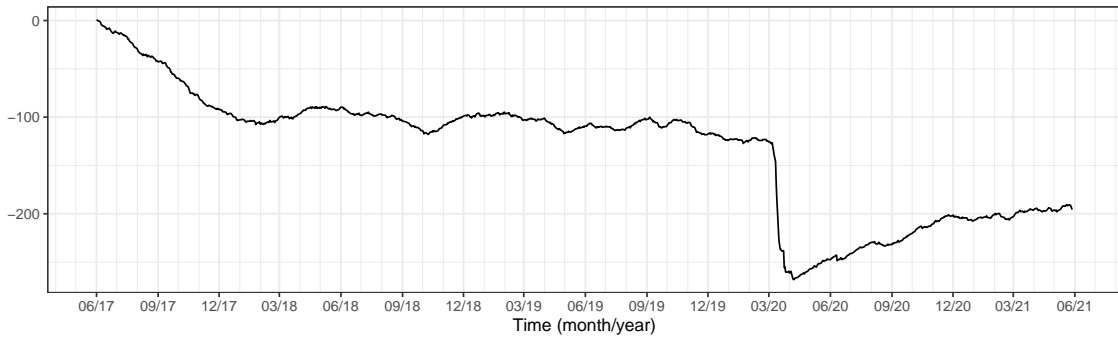


Figure 4.3: Relative log-likelihood

Overall, this analysis shows how a model with stochastic volatility is better at describing and predicting the considered time-frame of S&P500 returns. As can be seen from the graph and perhaps unsurprisingly, the density forecast given the stochastic volatility model represents a particularly significant improvement in the period of extreme values of returns in March 2020.

## 4.6 Realised volatility as benchmark

In section XX we compared several filtered distributions, briefly pointing out three main behaviours, namely that of the SIS algorithm, that of the Liu and West particle filter and that of the remaining filters. However, we did not have metrics that could help us clearly point at one behaviour as the closest to reality. In this section, we will employ realised volatility as one such metric.

A realised volatility measure - the realised variance based on 5 min intraday return intervals ($rv5$ series in the Oxford-Man Realized Library) - will be used as a proxy for the latent volatility process driving the log returns on the 3 indices presented in the earlier sections. As we previously mentioned, a transformation is needed as to compare filtered states and realised volatility, namely one turning both into estimates of the standard deviation of the percentage log returns. For each $t$, $rv5_t$ is then turned into $rv5_t^{0.5} * 100$, while $e^{x_t/2}$ (where $x_t$ is the filtered state) is computed by taking the mean of the generated particles and then applying the $exp(\cdot/2)$ transformation.

Throughout this section, we will deem as the best performing algorithm that coming closest to the proxy, either "literally" in a graphical framework or in a Root Mean Squared Error or Mean Absolute Error sense. Clearly enough, this approach builds on the assumption that realised variance is indeed a good proxy for latent volatility in real financial series.

A considerable amount of research in the 1990s and 2000s has focused on the properties of realised volatility measures, let them be realised variances or realised kernels. A thorough review of such literature can be found on the Oxford-Man Institute Realized volatility website, as their database specifically focuses these two measures.[22]

As Shephard and Sheppard (2010) themselves put it, in a paper that also presents the methodology that backs their Library, "such statistics are based on a variety of theoretically sound non-parametric estimators of the daily variation of prices". Thanks to their theoretical justification and their being model-free estimates, in

---

[22]Here we would mention the work by Barndorff-Nielsen and Shephard (2002), who focus on the asymptotic properties of the realised volatility error in stochastic volatility models, namely the difference between realized volatility and the "discretised integrated volatility", also called "actual volatility".

recent years realised volatility measures have been frequently used in financial applications as proxies for different types of latent volatility, providing a valuable (and arguably) preferable alternative to using squared returns (Hansen and Lunde, 2006).[23]

Nevertheless, we shall not indulge into forgetting the inherent limitations of using a proxy for a latent process. In particular, realised volatility should not be seen as a perfect proxy of latent volatility (as, for example, realised measures ignore overnight price variations), but rather as a comparatively solid one. Therefore, in this section conclusions will be drawn and put forward only when supported by large differences between models and filters, while we will keep a neutral stance when such support turns out to be mild.

### 4.6.1   Comparing the filters

In order to evaluate the different filters according to the evaluation tool represented by the realized volatility, we start once more from the visual inspection of the plots. For any of the three indices, below graphs are shown including both the filtered volatility obtained from the filtered states (for any of the Sequential MC methods described in the theoretical section) and the corresponding rescaled realised volatility series.[24] As compared to the visual analysis we conducted in section *fill with the number of the section*, we can now use such a proxy to determine the relative performance of the competing filters.

Once more, most algorithms used (aside from SIS and Liu-West) seem to provide indistinguishable results and, generally speaking, to underestimate the volatility (as indicated by the realised volatility proxy). The SIS algorithm appears completely inadequate to describe the "true" volatility process: as we argued in section XX, the degeneracy of its weights on the particles prevents it from delivering a good enough approximation of the target distribution (*check whether this is the correct intuition*). On top of that, it does not seem the case that the SIS algorithm, by falling short of the SV target distribution, ends up fitting the proxy better.[25]

On the other hand, the Liu and West filter offers the best performance among all filters, at least visually. This suggests that, since the Liu and West particle filter is built on a different underlying model than the other filters considered, this model may offer a better representation of the data analyzed. Once more, these considerations hold for all of the three indices.

---

[23]See for example Kambouroudis et al. (2016), Buncic and Gisler (2016), Gatheral et al.(2018), Allen and McAleer (2020), Guidolin and Pedio (2021).

[24]For simplicity,troughout the rest of this section we will omit "rescaled" when refering to the rescaled realised volatility.

[25]As we will now see, this seems instead to be the case for our preferred algorithms, namely those adopting adaptive resampling rules: a better approximation of the SV target filtering distribution yields slightly higher RMSEs and MAEs than those resulting from less accurate MC approximations.

GRAFICI

The above intuitions are confirmed by looking at Table XX, where the RMSE and MAE are shown for each filter (run with a number of particles equal to 10000), considering the realised volatility as benchmark. Indeed, for any index, most of the filters give rather similar results in terms of RMSE and MAE. For any index and for any measure, the worst performing is the SIS algorithm, while the best performing is the Liu and West particle filter. (Metterei qua l'intuizione del Liu West)

Table 4.5: RMSE and MAE, realised volatility as benchmark

|  | N | BPF | GPFOPT | APF | BAPF | LW | SIS |
|---|---|---|---|---|---|---|---|
| RMSE SP500 | 10000 | 0.5086 | 0.5093 | 0.5099 | 0.5103 | 0.4287 | 0.6029 |
| MAE SP500 | 10000 | 0.3538 | 0.3531 | 0.3517 | 0.3531 | 0.2916 | 0.4320 |
| RMSE STOXX | 10000 | 0.4636 | 0.4634 | 0.4757 | 0.4678 | 0.3441 | 0.6525 |
| MAE STOXX | 10000 | 0.3019 | 0.3042 | 0.3042 | 0.3042 | 0.2372 | 0.4408 |
| RMSE DJI | 10000 | 0.5076 | 0.5062 | 0.5093 | 0.5054 | 0.4408 | 0.6047 |
| MAE DJI | 10000 | 0.3375 | 0.3383 | 0.3374 | 0.3362 | 0.2810 | 0.4156 |

Finally, we can see from Table XX the RMSE and MAE obtained with a number of particles equal to 50000, for the SP500 and the EuroStoxx50 indices. We consider the Bootstrap particle filter and the Auxiliary particle filter, which we employed in section XX; in addition to these, we add the Liu and West filter, which did not feature in that section of this work.

In the case of the SP500 index, although the number of particles increases, the RMSE and MAE increase (although by very small amounts) for both the particle filters based on our usual specification of the SV model. Instead, for the Liu and West filter we see some improvements, although the small extent suggests that also the LW filter was already in the convergence phase with N=10000.

In the case of the EuroStoxx50 index, while the Bootstrap filter increases both RMSE and MAE when N is raised to 50000, the APF shows improvements in its performance, according to both criteria, which instead disagree for the Liu and West filter.

Table 4.6: RMSE and MAE, realised volatility as benchmark (SP500 and STOXX50E)

|             | N     | BPF     | APF     | LWF     |
|-------------|-------|---------|---------|---------|
| RMSE SP500  | 50000 | 0.51170 | 0.51489 | 0.42423 |
| MAE SP500   | 50000 | 0.35419 | 0.35534 | 0.29069 |
| RMSE STOXX  | 50000 | 0.46503 | 0.46704 | 0.34230 |
| MAE STOXX   | 50000 | 0.30344 | 0.30407 | 0.23956 |

Nevertheless, as we previously argued, we should not let tiny differences drive our conclusions. The idea behind employing also such 50000 particles approximations (*i.e* more precise and computationally expensive ones) is to check whether the relative performance that we assessed with N=10000 might be significantly influenced by issues of convergence among the filters: possibly, by further approaching the exact filtering distribution implied by the basic SV model, the filters built on such specification would improve their relative performance. This does not seem to be the case, even though the use of a proxy of the latent volatility process leaves room for discussion, as such conclusions rely on the assumption that such proxy is indeed a good one.[26] Rather, what this exercise highlights (under its assumptions) is a need for more flexibility and variability in the basic SV model: the underlying SV model of the LW filter meets this request, but clearly other solutions are possible, and have been argued for in the field of financial econometrics and mathematical finance, as we noted in the literary review section.

## 4.7   Bibliography

Allen, D. E., & McAleer, M. (2020). Do we need stochastic volatility and generalised autoregressive conditional heteroscedasticity? Comparing squared end-of-day returns on FTSE. Risks, 8(1), 12.

Allen, D. E. (2020). Stochastic Volatility and GARCH: Do Squared End-of-Day Returns Provide Similar

---

[26]Nota che riporta il fatto che in certi casi si ottengano MAE e RMSE più bassi usando N più bassi di 10000: in altre parole, approssimare un po' peggio la distribuzione implicata dal modello SV può portare a rispettare meglio la proxy.

Information?. Journal of Risk and Financial Management, 13(9), 202.

Andrieu, C., Doucet, A., & Holenstein, R. (2010). Particle markov chain monte carlo methods. Journal of the Royal Statistical Society: Series B (Statistical Methodology), 72(3), 269-342.

Barndorff-Nielsen, O. E., & Shephard, N. (2001). Non-Gaussian Ornstein–Uhlenbeck-based models and some of their uses in financial economics. Journal of the Royal Statistical Society: Series B (Statistical Methodology), 63(2), 167-241.

Barndorff-Nielsen, O. E., & Shephard, N. (2002). Econometric analysis of realized volatility and its use in estimating stochastic volatility models. Journal of the Royal Statistical Society: Series B (Statistical Methodology), 64(2), 253-280.

Bollerslev, T. (1986). Generalized autoregressive conditional heteroskedasticity. Journal of econometrics, 31(3), 307-327.

Breidt, F. J., Crato, N., & De Lima, P. (1998). The detection and estimation of long memory in stochastic volatility. Journal of econometrics, 83(1-2), 325-348.

Buncic, D., & Gisler, K. I. (2016). Global equity market volatility spillovers: A broader role for the United States. International Journal of Forecasting, 32(4), 1317-1339.

Chan, J. C. (2013). Moving average stochastic volatility models with application to inflation forecast. Journal of Econometrics, 176(2), 162-172.

Chib, S., Nardari, F., & Shephard, N. (2002). Markov chain Monte Carlo methods for stochastic volatility models. Journal of Econometrics, 108(2), 281-316.

Chib, S., Nardari, F., & Shephard, N. (2006). Analysis of high dimensional multivariate stochastic volatility

models. Journal of Econometrics, 134(2), 341-371.

Chopin, N., & Papaspiliopoulos, O. (2020). An introduction to sequential Monte Carlo (Vol. 4). Springer.

Comte, F., & Renault, E. (1998). Long memory in continuous-time stochastic volatility models. Mathematical finance, 8(4), 291-323.

Christoffersen, P., Jacobs, K., & Mimouni, K. (2010). Volatility dynamics for the S&P500: Evidence from realized volatility, daily returns, and option prices. The Review of Financial Studies, 23(8), 3141-3189.

Dimitrakopoulos, S., & Kolossiatis, M. (2020). Bayesian analysis of moving average stochastic volatility models: modeling in-mean effects and leverage for financial time series. Econometric Reviews, 39(4), 319-343.

Douc, R., Moulines, E., & Stoffer, D. (2014). Nonlinear time series: Theory, methods and applications with R examples. CRC press.

Engle, R. F. (1982). Autoregressive conditional heteroscedasticity with estimates of the variance of United Kingdom inflation. Econometrica: Journal of the econometric society, 987-1007.

Eraker, B. (2004). Do stock prices and volatility jump? Reconciling evidence from spot and option prices. The Journal of Finance, 59(3), 1367-1403.

Friz, P. K., Gassiat, P., & Pigato, P. (2021). Precise asymptotics: robust stochastic volatility models. The Annals of Applied Probability, 31(2), 896-940.

Gatheral, J., Jaisson, T., & Rosenbaum, M. (2018). Volatility is rough. Quantitative finance, 18(6), 933-949.

Guidolin, M., & Pedio, M. (2021). Media Attention vs. Sentiment as Drivers of Conditional Volatility Predictions: An Application to Brexit. Finance Research Letters, 101943.

Hansen, P. R., & Lunde, A. (2006). Consistent ranking of volatility models. Journal of Econometrics, 131(1-2), 97-121.

Harvey, A. C., & Shephard, N. (1996). Estimation of an asymmetric stochastic volatility model for asset returns. Journal of Business & Economic Statistics, 14(4), 429-434.

Harvey, A., Ruiz, E., & Shephard, N. (1994). Multivariate stochastic variance models. The Review of Economic Studies, 61(2), 247-264.

Heber, Gerd, Asger Lunde, Neil Shephard and Kevin Sheppard (2009). Oxford-Man Institute's realized library. Oxford-Man Institute, University of Oxford, version 0.3. Available at: https://realized.oxford-man.ox.ac.uk/.

Heston, S. L. (1993). A closed-form solution for options with stochastic volatility with applications to bond and currency options. The review of financial studies, 6(2), 327-343.

Hull, J., & White, A. (1987). The pricing of options on assets with stochastic volatilities. The journal of finance, 42(2), 281-300.

Jacquier, E., Polson, N. G., & Rossi, P. (1994). Bayesian analysis of stochastic volatility models. Journal of Business and Economic Statistics, 12(4), 371-389.

Jacquier, E., Polson, N. G., & Rossi, P. E. (2004). Bayesian analysis of stochastic volatility models with fat-tails and correlated errors. Journal of Econometrics, 122(1), 185-212.

Johannes, M., Evers, L. (2007). Monte Carlo Methods. Lecture Notes. University of Bristol, Department of Mathematics.

Johannes, M., Korteweg, A., & Polson, N. (2014). Sequential learning, predictability, and optimal portfolio

returns. The Journal of Finance, 69(2), 611-644.

Kambouroudis, D. S., McMillan, D. G., & Tsakou, K. (2016). Forecasting stock return volatility: a comparison of GARCH, Implied volatility, and realized volatility models. Journal of Futures Markets, 36(12), 1127-1163.

Kastner, G. (2019). Dealing with stochastic volatility in time series using the R package stochvol. arXiv preprint arXiv:1906.12134.

Kim, S., Shephard, N., & Chib, S. (1998). Stochastic volatility: likelihood inference and comparison with ARCH models. The review of economic studies, 65(3), 361-393.

Kim, J., & Stoffer, D. S. (2008). Fitting stochastic volatility models in the presence of irregular sampling via particle methods and the EM algorithm. Journal of time series analysis, 29(5), 811-833.

Koopman, S. J., & Hol Uspensky, E. (2002). The stochastic volatility in mean model: empirical evidence from international stock markets. Journal of applied Econometrics, 17(6), 667-689.

Liesenfeld, R., & Jung, R. C. (2000). Stochastic volatility models: conditional normality versus heavy-tailed distributions. Journal of applied Econometrics, 15(2), 137-160.

Luo, R., Zhang, W., Xu, X., & Wang, J. (2018, April). A neural stochastic volatility model. In Thirty-second AAAI conference on artificial intelligence.

Mao, X., Czellar, V., Ruiz, E., & Veiga, H. (2020). Asymmetric stochastic volatility models: Properties and particle filter-based simulated maximum likelihood estimation. Econometrics and Statistics, 13, 84-105.

Nakajima, J., & Omori, Y. (2012). Stochastic volatility model with leverage and asymmetrically heavy-tailed error using GH skew Student's t-distribution. Computational Statistics & Data Analysis, 56(11), 3690-3704.

Omori, Y., Chib, S., Shephard, N., & Nakajima, J. (2007). Stochastic volatility with leverage: Fast and efficient likelihood inference. Journal of Econometrics, 140(2), 425-449.

Petris, G., Petrone, S., Campagnali, P. (2010). Dynamic Linear Models with R. Springer.

Pitt, M. K., & Shephard, N. (1999). Filtering via simulation: Auxiliary particle filters. Journal of the American statistical association, 94(446), 590-599.

Poon, S. H., & Granger, C. (2005). Practical issues in forecasting volatility. Financial analysts journal, 61(1), 45-56.

Shephard, N., & Sheppard, K. (2010). Realising the future: forecasting with high-frequency-based volatility (HEAVY) models. Journal of Applied Econometrics, 25(2), 197-231.

So, M. E. P., Lam, K., & Li, W. K. (1998). A stochastic volatility model with Markov switching. Journal of Business & Economic Statistics, 16(2), 244-253.

Xu, X., & Chen, Y. (2021). Deep Stochastic Volatility Model. arXiv preprint arXiv:2102.12658.

Zhang, B., Chan, J. C., & Cross, J. L. (2020). Stochastic volatility models with ARMA innovations: An application to G7 inflation forecasts. International Journal of Forecasting, 36(4), 1318-1328.

# Chapter 5

# Appendix

## 5.1 The Stochastic Volatility Model

We decide to organise this Appendix as an R package. All the R functions described in this Appendix take as reference a basic specification of Stochastic Volatility Model.

$$y_t|x_t \sim N(0, e^{x_t})$$

$$x_t|x_{t-1}, \alpha, \beta, \tau^2 \sim N(\alpha + \beta x_{t-1}, \tau^2)$$

All the plots and tables of this work concerning stochastic volatility models use this functions.

```
SVPFfun(data,N,m0,C0,alpha,beta,tau,r)
```

**Arguments**

data   the observed process. It has to be a vector or a univariate time series.

N   number of particles generated at each step

m0   central value of the normal prior state distribution

C0   variance of the normal prior state distribution

alpha   intercept $\alpha$ in the state equation

beta   coefficient $\beta$ in the state equation

r   if present the threshold is set equal to $N/r$ otherwise, if missing, the threshold is set equal to $N/2$

```r
SVPFfun<-function(data,N,m0,C0,alpha,beta,tau,r){
  if(missing(r)){r=2}else{}
  xs<-NULL
  ws<-NULL
  ess<-NULL
  x  = rnorm(N,m0,sqrt(C0))
  w  = rep(1/N,N)


  for(t in 1:length(data)){

    x<-rnorm(N,alpha+beta*x,tau)
    w1<-w*dnorm(data[t],0,exp(x/2))


    w = w1/sum(w1)
    ESS  = 1/sum(w^2)


    if(ESS<(N/r)){
      index<-sample(N,size=N,replace=T,prob=w)
      x<-x[index]
      w<-rep(1/N,N)
    }else{}

    xs = rbind(xs,x)
    ws = rbind(ws,w)
    ess =rbind(ess,ESS)
  }
  return(list(xs=xs,ws=ws,ess=ess))
}
```

```r
SVGPFfun(data,N,m0,C0,alpha,beta,tau,r)
```

**Arguments**

`data`  the observed process. It has to be a vector or a univariate time series.

`N`  number of particles generated at each step

`m0`  central value of the normal prior state distribution

`C0`  variance of the normal prior state distribution

`alpha`  intercept $\alpha$ in the state equation

`beta`  coefficient $\beta$ in the state equation

`r`  if present the threshold is set equal to $N/r$ otherwise, if missing, the threshold is set equal to $N/2$

```r
SVGPFfun<-function(data,N,m0,C0,alpha,beta,tau,r){

  if(missing(r)){r=2}else{}
  xs<-NULL
  ws<-NULL
  ess<-NULL
  x  = rnorm(N,m0,sqrt(C0))
  w  = rep(1/N,N)


  for(t in 1:length(data)){


    xprev<-x
    x<-rnorm(N,alpha+beta*x+(tau^2)/4*((data[t]^2)*exp(-(alpha+beta*x))-2),tau)
    w1<-w*dnorm(data[t],0,exp(x/2))*dnorm(x,alpha+beta*xprev,tau)/
      dnorm(x,mean=alpha+beta*xprev+(tau^2)/4*((data[t]^2)*exp(-(alpha+beta*xprev))-2),tau)


    w = w1/sum(w1)
    ESS  = 1/sum(w^2)


    if(ESS<(N/r)){
      index<-sample(N,size=N,replace=T,prob=w)
      x<-x[index]
      w<-rep(1/N,N)
    }else{}
```

```
    xs = rbind(xs,x)

    ws = rbind(ws,w)

    ess =rbind(ess,ESS)

  }

  return(list(xs=xs,ws=ws,ess=ess))

}
```

---

SVAPFfun(data,N,m0,C0,alpha,beta,tau,r)

---

**Arguments**

`data`  the observed process. It has to be a vector or a univariate time series.

`N`  number of particles generated at each step

`m0`  central value of the normal prior state distribution

`C0`  variance of the normal prior state distribution

`alpha`  intercept $\alpha$ in the state equation

`beta`  coefficient $\beta$ in the state equation

`r`  if present the threshold is set equal to $N/r$ otherwise, if missing, the threshold is set equal to $N/2$

```
SVAPFfun<-function(data,N,m0,C0,alpha,beta,tau,r){

  if(missing(r)){r=2}else{}

  xs<-NULL

  ws<-NULL

  ess<-NULL

  x  = rnorm(N,m0,sqrt(C0))

  w  = rep(1/N,N)


  for(t in 1:length(data)){


    weight = w*dnorm(data[t],0,exp(x/2))

    k    = sample(1:N,size=N,replace=TRUE,prob=weight)

    x1   = rnorm(N,alpha+beta*x[k],tau)
```

```
    lw  = dnorm(data[t],0,exp(x1/2),log=TRUE)-dnorm(data[t],0,exp(x[k]/2),log=TRUE)

    w   = exp(lw)

    w   = w/sum(w)

    ESS = 1/sum(w^2)


    if(ESS<(N/r)){

      index<-sample(N,size=N,replace=T,prob=w)

      x<-x1[index]

      w<-rep(1/N,N)

    }else{}


    x <- x1

    xs = rbind(xs,x)

    ws = rbind(ws,w)

    ess =rbind(ess,ESS)


  }
  return(list(xs=xs,ws=ws,ess=ess))
}
```

SVAPFoptfun(data,N,m0,C0,alpha,beta,tau,r)

**Arguments**

data   the observed process. It has to be a vector or a univariate time series.

N   number of particles generated at each step

m0   central value of the normal prior state distribution

C0   variance of the normal prior state distribution

alpha   intercept $\alpha$ in the state equation

beta   coefficient $\beta$ in the state equation

r   if present the threshold is set equal to $N/r$ otherwise, if missing, the threshold is set equal to $N/2$

```
SVAPFoptfun<-function(data,N,m0,C0,alpha,beta,tau,r){

  if(missing(r)){r=2}else{}

  xs<-NULL
```

```r
  ws<-NULL
  ess<-NULL
  x  = rnorm(N,m0,sqrt(C0))
  w  = rep(1/N,N)


  for(t in 1:length(data)){
    x_prev=x
    x_hat = alpha+beta*x #means of the transition from the previous particle
    I_k = sample(1:N,prob=w*dnorm(data[t],0,sqrt(exp((x_hat)/2))))
    for(k in 1:N){
      x[k]=rnorm(size=1,mean=alpha+beta*x_prev[I_k],sd=tau)
      w[k]=dnorm(data[t],0,sqrt(exp((x[k])/2)))/dnorm(data[t],0,sqrt(exp((x_hat)/2)))
    }
    w = w/sum(w)
    ESS  = 1/sum(w^2)


    if(ESS<(N/r)){
      index<-sample(N,size=N,replace=T,prob=w)
      x<-x[index]
      w<-rep(1/N,N)
    }else{}


    xs = rbind(xs,x)
    ws = rbind(ws,w)
    ess =rbind(ess,ESS)


  }
  return(list(xs=xs,ws=ws,ess=ess))
}
```

```r
SVLWfun(data,N,m0,C0,ealpha,valpha,ebeta,vbeta,nu,lambda)
```

**Arguments**

data   the observed process. It has to be a vector or a univariate time series.

N   number of particles generated at each step

m0   central value of the normal prior state distribution

C0   variance of the normal prior state distribution

alpha   intercept $\alpha$ in the state equation

beta   coefficient $\beta$ in the state equation

r   if present the threshold is set equal to $N/r$ otherwise, if missing, the threshold is set equal to $N/2$

```r
SVLWfun<-function(data,N,m0,C0,ealpha,valpha,ebeta,vbeta,nu,lambda){

  xs  = rnorm(N,m0,sqrt(C0))
  pars   = cbind(rnorm(N,ealpha,sqrt(valpha)),rnorm(N,ebeta,sqrt(vbeta)),
                 log(1/rgamma(N,nu/2,nu*lambda/2)))
  delta  = 0.75
  a      = (3*delta-1)/(2*delta)
  h2     = 1-a^2
  parss  = array(0,c(N,3,n))
  xss    = NULL
  ws     = NULL
  ESS    = NULL
  w      = rep(1/N,N)
  vpars   = NULL
  for (t in 1:length(data)){

    #mpar          = apply(pars,2,mean) #alternatively use this
    mpar<-c()
    for(i in 1:3){
      mpar[i]    = weighted.mean(pars[,i],w)
    }

    vpar      = var(pars)
    ms            = a*pars+(1-a)*matrix(mpar,N,3,byrow=T)
    mus           = pars[,1]+pars[,2]*xs
    weight        = w*dnorm(data[t],0,exp(mus/2))
```

```r
    k              = sample(1:N,size=N,replace=T,prob=weight)

    ms1            = ms[k,] + matrix(rnorm(3*N),N,3)%*%chol(h2*vpar)

    xt             = rnorm(N,ms1[,1]+ms1[,2]*xs[k],exp(ms1[,3]/2))

    w              = dnorm(data[t],0,exp(xt/2))/dnorm(data[t],0,exp(mus[k]/2))

    w              = w/sum(w)

    ESS            = 1/sum(w^2)



    if(ESS<(N/2)){

      index<-sample(N,size=N,replace=T,prob=w)

      xs<-xt[index]

      pars<-ms1[index,]

      w<-rep(1/N,N)

    }else{

      xs<-xt

      pars<-ms1

    }


    vpars           = rbind(vpars,vpar)

    xss            = rbind(xss,xs)

    parss[,,t]    = pars

    ws             = rbind(ws,w)

  }

  return(list(xs=xss,pars=parss,ws=ws,vpars=vpars))

}
```

---

```r
SISfun(data,N,m0,C0,alpha,beta,tau,r)
```

---

**Arguments**

`data`  the observed process. It has to be a vector or a univariate time series.

`N` number of particles generated at each step

`m0` central value of the normal prior state distribution

`C0` variance of the normal prior state distribution

`alpha` intercept $\alpha$ in the state equation

`beta` coefficient $\beta$ in the state equation

`r` if present the threshold is set equal to $N/r$ otherwise, if missing, the threshold is set equal to $N/2$

```
SISfun<-function(data,N,m0,C0,alpha,beta,tau,r){
  if(missing(r)){r=2}else{}
  xs<-NULL
  ws<-NULL
  ess<-NULL
  x  = rnorm(N,m0,sqrt(C0))
  w  = rep(1/N,N)


  for(t in 1:length(data)){


    x<-rnorm(N,alpha+beta*x,tau)
    w1<-w*dnorm(data[t],0,exp(x/2))


    w = w1/sum(w1)
    ESS  = 1/sum(w^2)


    if(ESS<0){
      index<-sample(N,size=N,replace=T,prob=w)
      x<-x[index]
      w<-rep(1/N,N)
    }else{}


    xs = rbind(xs,x)
    ws = rbind(ws,w)
    ess =rbind(ess,ESS)
```

```
  }
  return(list(xs=xs,ws=ws,ess=ess))
}
```

---

```
BAPFfun(data,N,m0,C0,alpha,beta,tau,r)
```

---

**Arguments**

data   the observed process. It has to be a vector or a univariate time series.

N   number of particles generated at each step

m0   central value of the normal prior state distribution

C0   variance of the normal prior state distribution

alpha   intercept $\alpha$ in the state equation

beta   coefficient $\beta$ in the state equation

r   if present the threshold is set equal to $N/r$ otherwise, if missing, the threshold is set equal to $N/2$

---

```
BAPFfun<-function(data,N,m0,C0,alpha,beta,tau,r){
  if(missing(r)){r=2}else{}
  xs<-NULL
  ws<-NULL
  ess<-NULL
  x   = rnorm(N,m0,sqrt(C0))
  w   = rep(1/N,N)


  for(t in 1:length(data)){


    x<-rnorm(N,alpha+beta*x,tau)
    w1<-w*dnorm(data[t],0,exp(x/2))


    w = w1/sum(w1)
```

```r
    ESS  = 1/sum(w^2)


    if(ESS>-1){
      index<-sample(N,size=N,replace=T,prob=w)
      x<-x[index]
      w<-rep(1/N,N)
    }else{}


    xs = rbind(xs,x)
    ws = rbind(ws,w)
    ess =rbind(ess,ESS)
  }
  return(list(xs=xs,ws=ws,ess=ess))
}
```